SYNTHESES AND CHARACTERIZATION OF POLYMERIC NANOCOMPOSITES PREPERAD BY IN-SITU PHOTOPOLYMERIZATION

by

ALPER NEŞE

B.S., Chemistry, Hacettepe University, 2004

Submitted to the Institute for Graduate Studies in
Science and Engineering in partial fulfillment of the
requirements for the degree of
Master of Science

Graduate Program in Chemistry
Boğaziçi University
2006

SYNTHESES AND CHARACTERIZATION OF POLYMERIC NANOCOMPOSITES PREPARED BY IN-SITU PHOTOPOLYMERIZATION

APPROVED BY:

Prof. Nihan Nugay . . . . . .
(Thesis Supervisor)

Dr. Mutlu Kartın . . . .

Prof. Yusuf Yağcı . . . .

DATE OF APPROVAL:

ACKNOWLEDGEMENTS

I would like to express my sincere gratitude to Prof. Nihan Nugay for giving me the opportunity to join her research group to conduct this project which in turn gave me the chance to publish my first paper. I am also thankful for her guidence through my master studies.

I would like to express my special thanks to Prof. Yusuf Yağcı for his guidence through my project and the advises he has given me on my scientific career. It was a great honour to work with him on my thesis.

I would like to express my thanks to one of the thesis committee member, Dr. Mutlu Kartın for reviewing my thesis as well as making helpful comments on it.

I would like to thank to Mehmet Atilla Taşdelen for his help on the experimental part and for giving me advises; Dr. Sinan Şen for his guidence and help in the laboratory; Gökhan Çaylı, Dr. Bilge Gedik, Aslı Çakır and Assoc. Prof. Seyhun Solakoğlu for their help to obtain Thermogravimetric Analyses (TGA), Scanning Electron Microscopy (SEM), X-Ray Diffraction (XRD) and Transmission Electron Microscopy (TEM) data, respectively; Hülya Metiner for her guidence in the department; and to all members of the chemistry department for their encouragement and moral support during my master study.

ABSTRACT

SYNTHESES AND CHARACTERIZATION OF POLYMERIC NANOCOMPOSITES PREPERAD BY IN-SITU PHOTOPOLYMERIZATION

In this project, the objective was to synthesize a nanocomposite with a photoinitiator acting intercalent. With this motivation, in-situ syntheses of poly(methyl methacrylate) (PMMA) nanocomposites by photopolymerization using organophilic montmorillonite (MMT) as the layered clay, is reported. MMT clay was ion-exchanged with N-phenacyl, N,N-dimethylanilinium hexafluoro phosphate (PDA) which acts as both suitable intercalent and photoinitiator. The modified clay (MC) was then dispersed in methyl methacrylate (MMA) monomer in different loading degrees to carry out the in-situ photopolymerization. Two of the resulting nanocomposites obtained from the MC, the PMMA nanocomposite which was synthesized by using 3 % MC (PMMA-3%MC) and the PMMA nanocomposite which was synthesized by using 5 % MC (PMMA-5%MC) were found to result in a further increase in the d-spacings of the MMT layers at the value of 3.37 Å and 3.63 Å, respectively. On the other hand, for the PMMA nanocomposite which was synthesized by using 1 % MC (PMMA-1%MC), no d_{001} reflection was observed in the XRD patterns indicating complete exfoliated structure. It was also proved that PDA was organophilic enough to allow polymerization between clay layers. Intercalation ability of the photoinitiator and exfoliated nanocomposite structures were proved by both XRD and TEM. It was seen that even with 1 % degree of loading, the desired exfoliation was reached. Thermal properties were studied by using DSC and TGA. It was observed that the nanocomposite with exfoliated structure had the highest glass transition temperature (T_g) and thermal stability. Exfoliation-intercalation morphology of the resultant polymeric nanocomposites was also examined by using SEM and the results were discussed.

ÖZET

İN-SİTU FOTOPOLİMERİZASYON YÖNTEMİ İLE HAZIRLANAN POLİMERİK NANOKOMPOZİTLERİN SENTEZİ VE KARAKTERİZASYONU

Bu projede, aynı zamanda bir interkelant olarakta davranan bir fotobaşlatıcı kullanarak polimer-kil nanokompozitlerinin sentezi amaçlandı. Bu motivasyonla, polimetilmetakrilat (PMMA) nanokompozitlerinin in-situ sentezi, organofilik montmorillonit kili (MMT) kullanılarak fotopolimerizasyon ile gerçekleştirildi. İlk olarak, MMT kili, uygun bir interkelant ve foto-başlatıcı olan N-fenaçil, N,N-dimetillanilinyum hekzaflorofosfat (PDA) ile iyon değişimine uğratıldı. Daha sonra bu modifiye kil metilmetakrilat (MMA) monomerinin içine farklı yükleme derecelerinde dağıtılarak in-situ fotopolimerizasyon gerçekleştirildi. Modifiye kilden (MC) elde edilen nanokompozitlerin ikisi olan, % 3 MC kullanılarak sentezlenen PMMA nanokompozitinin (PMMA-3%MC) ve % 5 MC kullanılarak sentezlenen PMMA nanokompozitinin (PMMA-5%MC), MMT tabakalarının arasındaki mesafenin sırasıyla 3.37 Å ve 3.63 Å artmasına sebep olduğu bulundu. Bununla beraber, % 1 MC kullanılarak sentezlenen PMMA nanokompozitinin (PMMA-1%MC) X-ışınları difraktogramlarındaki d_{001} yansıtmasının yokluğu ile bu kompozitin tamamıyla eksfoliye bir yapıya sahip olduğu sonucuna varıldı. Fotobaşlatıcının interkelasyon özelliği ve eksfoliye nanokompozitlerin yapısı, XRD ve TEM ile kanıtlandı. Termal özellikler, DSC ve TGA kullanılarak incelendi. Eksfoliye yapıya sahip nanokompozitin en yüksek camsı geçiş sıcaklığına (T_g) ve en iyi termal kararlılığa sahip olduğu görüldü. Elde edilen nanokompozitlerin eksfoliasyon-interkelasyon morfolojileri SEM ile de incelendi ve tartışıldı.

TABLE OF CONTENTS

LIST OF FIGURES

LIST OF TABLES

LIST OF SYMBOLS\ABBREVIATIONS

ΔG	The Change in Gibbs Free Energy
T_g	Glass Transition Temperature
^{1}H-NMR	Proton Nuclear Magnetic Resonance Spectroscopy
CCD	Charge Coupled Device
CEC	Cation Exchange Capacity
COI	Coinitiator
DMA	Dynamic Mechanical Analyses
EDAX	Energy Dispersive Analyses of X-Ray
FTIR	Fourier Transform Infrared Spectroscopy
MC	Modified Clay
MMA	Methylmethacrylate
MMT	Montmorillonite
OMLS	Organically Modified Layered Silicate
PDA	N-phenacyl, N,N-dimethylanilinium hexafluoro phosphate
PLS	Polymer/Layered Silicate
PMMA	Polymethylmethacrylate
PMMA-1%MC	PMMA Nanocomposite Including 1 % Modified Clay
PMMA-3%MC	PMMA Nanocomposite Including 3 % Modified Clay
PMMA-5%MC	PMMA Nanocomposite Including 5 % Modified Clay
RTIR	Real Time Infrared Spectroscopy
SEM	Scanning Electron Microscopy
TEM	Transmission Electron Microscopy
TGA	Thermogravimetric Analysis
UV	Ultraviolet
WAXD	Wide Angle X-Ray Diffraction
XRD	X-Ray Diffraction

1. INTRODUCTION

1.1. Polymeric Nanocomposites

The nanocomposite approach has advantages over traditional fiber reinforced composites in the low filler loading range. Despite this, the market for high-performance fiber reinforced composites with high fiber volume fractions has not been affected by these developments.

The mystery of the 'nano-world' has been progressively exposed in recently years. The nanometer scale is simply a range between micro and molecular dimensions. The sciences in these two dimensional ranges have been well explored by materials scientists and chemists. Materials science and chemistry are often engaged in research on the nanometer scale, for example, the dimensions of crystal structures. The well-known nanometer-scale technologies which have been developed within materials science and chemistry in the past, may not be reasonably regarded as nanotechnology. The real interest in nanotechnology is to create revolutionary properties and functions by tailoring materials and designing devices on the nanometer scale.

Clay/polymer nanocomposites are a typical example of nanotechnology. This class of material uses smectite-type clays, such as hectorite, MMT, and synthetic mica, as fillers to enhance the properties of polymers. Smectite-type clays have layered structures. Each layer is constructed from tetrahedrally coordinated silicon atoms fused into an edge-shared octahedral plane of either $Al(OH)_3$ or $Mg(OH)_2$. According to the nature of the bonding between these atoms, the layers should exhibit excellent mechanical properties parallel to the layer direction. However, the exact mechanical properties of the layers are not yet known. It has been estimated from recent modeling work that the Young's modulus in the layer direction is 50 to 400 times higher than that of a typical polymer [1-5]. The layers have a high aspect ratio and each one is approximately 1 nm thick, while the diameter may vary from 30 nm to several microns or larger [6]. Hundreds or thousands of these layers are stacked together with weak Van der Waals forces to form a clay particle. With such a configuration, it is possible to tailor clays into various different structures in a polymer.

In the past, the major interest in using clays for polymer enhancement was to break down clay particle, which aggregates into individual particles to form micro-sized filler reinforced polymers, as shown in Figure 1.1. It can be imagined that the excellent mechanical properties of each individual layer in clay particles cannot function effectively in a such system. The weak interlayer bonding may act as damage initiation sites in applications. It is common to use high clay loading to achieve adequate improvement of the modulus, while strength and toughness of the polymer are reduced.

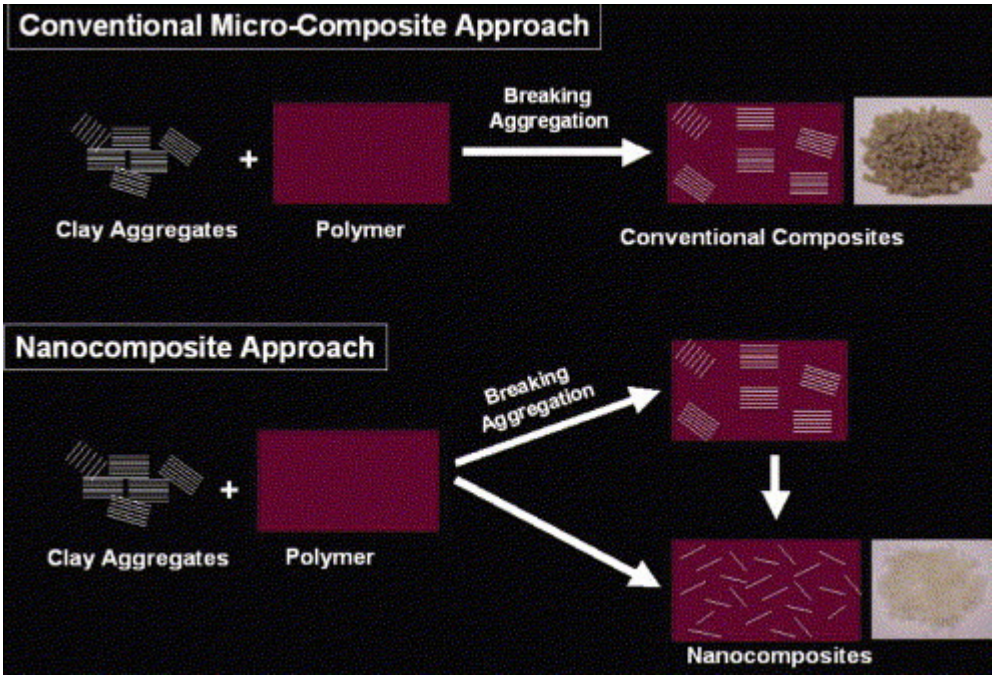

Figure 1.1. The different principles applied to the fabrication of conventional microcomposites and nanocomposites [5]

The principle used in clay/polymer nanocomposites is to separate not only clay aggregates but also individual silicate layers in a polymer, as illustrated schematically in Figure 1.1. By doing this, the excellent mechanical properties of the individual clay layers can function effectively, while the number of reinforcing components also increases dramatically because each clay particle contains hundreds or thousands of layers. As a consequence, a wide range of engineering properties can be significantly improved with a low level of filler loading, typically less than 5 weight %. At such a low loading level, polymers such as nylon-6 show an increase in Young's modulus of 103 %, in tensile strength of 49 %, and in heat distortion temperature of 146 % [7]. Other improved physical

and engineering properties include fire retardancy [8-9], barrier resistance [10-12], and ion conductivity [13-14].

Another advantage of clay/polymer nanocomposites is that the optical properties of the polymer are not significantly affected. The thickness of individual clay layers is much smaller than the wavelength of visible light so that well exfoliated clay/polymer nanocomposites should be optically clear. The images of micro- and nano-composites shown in Figure 1.1 were produced using the same clay and polypropylene mixture and applying a rapid cooling processes to minimize the crystallization effect. The conventional microcomposites appear brown and opaque, while the nanocomposites are almost transparent.

It is clear from this evidence that clay/polymer nanocomposites are a good demonstration of nanotechnology. By tailoring the clay structure in polymers on the nanometer scale, novel material properties have been found. Another interest in developing clay/polymer nanocomposites is that the technology can be applied immediately for commercial applications, while most other nanotechnologies are still in the concept and proving stage.

The first commercial application of these materials was the use of clay/nylon-6 nanocomposites as timing belt covers for Toyota cars, in collaboration with Ube in 1991 [15]. Shortly after this, Unitika introduced nylon-6 nanocomposites for engine covers on Mitsubishi's GDI engines [15]. In August 2001, General Motors and Basell announced the application of clay/polyolefin nanocomposites as a step assistant component for GMC Safari and Chevrolet Astro vans [16]. This was followed by the application of these nanocomposites in the doors of Chevrolet Impalas [16]. More recently, Noble Polymers has developed clay/polypropylene nanocomposites for structural seat backs in the Honda Acura [17], while Ube is developing clay/nylon-12 nanocomposites for automotive fuel lines and fuel system components.

In addition to automotive applications, clay/polymer nanocomposites have been used to improve barrier resistance in beverage applications. Alcoa CSI has applied multilayer clay/polymer nanocomposites as barrier liner materials for enclosure applications [18]. Honeywell has developed commercial clay/nylon-6 nanocomposite

products, Aegis™ NC resin, for drink packaging applications [19]. More recently, Mitsubishi Gas Chemical and Nanocor have developed Nylon-MXD6 nanocomposites for multilayered polyethylene terephthalate PET bottle applications [20].

1.1.1. Structure and Properties of Layered Silicates

The commonly used layered silicates for the preparation of polymer layered silicate (PLS) nanocomposites belong to the same general family of 2:1 of layered or phyllosilicates. Their crystal structure consists of layers made up of two tetrahedrally coordinated silicon atoms fused to an edge-shared octahedral sheet of either aluminum or magnesium hydroxide. The layer thickness is around 1 nm, and the lateral dimensions of these layers may vary from 30 nm to several microns or larger, depending on the particular layered silicate. Stacking of the layers leads to a regular Van der Waals gap between the layers called the interlayer or gallery. Isomorphic substitution within the layers (for example, Al^{3+} replaced by Mg^{2+} or Fe^{2+}, or Mg^{2+} replaced by Li^{+}) generates negative charges that can be counterbalanced by alkali and alkaline earth cations situated inside the galleries. This type of layered silicate is characterized by a moderate surface charge known as the Cation Exchange Capacity (CEC), and generally expressed as meq./100 g. This charge is not locally constant, but varies from layer to layer, and must be considered as an average value over the whole crystal structure.

MMT, hectorite, and saponite are one of the most commonly used layered silicates. Layered silicates have two types of structure of which tetrahedraly substituted and octahedraly substituted. In the case of tetrahedrally substituted layered silicates the negative charge is located on the surface of silicate layers, and hence, the polymer matrices can interact more readily with these than with octahedrally-substituted ones. Details regarding the structure and chemistry for these layered silicates are provided in Figure 1.2 and Table 1.1, respectively.

Two particular characteristics of layered silicates are generally considered for PLS nanocomposites. The first one is the ability of the silicate particles to disperse into individual layers and the second characteristic of it is the ability to fine-tune on their surface chemistry through ion exchange reactions with organic and inorganic cations.

Effect of interlayer cation on the degree of dispersion of the layered silicate in a particular matrix makes these two characteristics interrelated.

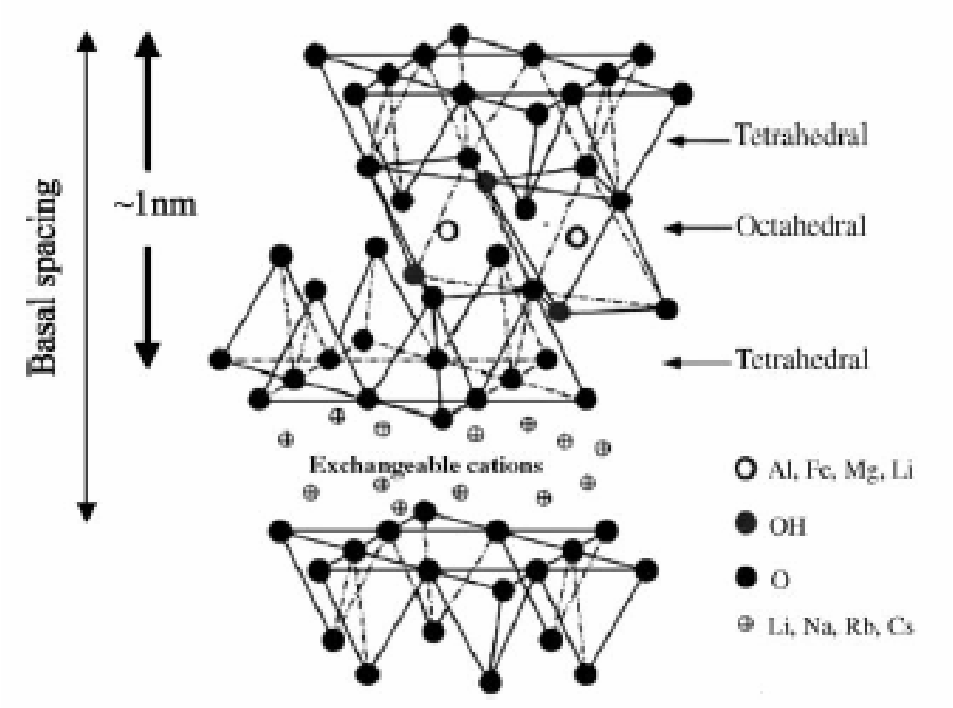

Figure 1.2. Structure of 2:1 phyllosilicates [6]

Table 1.1. Chemical formulae of commonly used 2:1 phyllosilicates

2:1 Phyllosilicate	General Formula	CEC(meq./100 g)	Particlelength (nm)
MMT	$M_x(Al_{4-x}Mg_x)Si_8O_{20}(OH)_4$	110.0	100-150
Hectorite	$M_x(Al_{6-x}Mg_x)Si_8O_{20}(OH)_4$	120.0	200-300
Saponite	$M_xMg_6(Si_{8-x}Al_x)O_{20}(OH)_4$	86.6	50-60

M= monovalent cation; x = degree of isomorphous substitution (between 0.5 and 1.3)

1.1.2. Structure and Properties of Organically Modified Layered Silicates (OMLS)

The physical mixture of a polymer and layered silicate may not form a nanocomposite. This situation is analogous to polymer blends, and in most cases separation into discrete phases takes place. In immiscible systems, which typically correspond to the more conventionally filled polymers, the poor physical interaction between the organic and the inorganic components leads to poor mechanical and thermal properties. In contrast, strong interactions between the polymer and the layered silicate in PLS nanocomposites lead to the organic and inorganic phases being dispersed at the nanometer level. As a result, nanocomposites exhibit unique properties that are not shared by their micro counterparts or conventionally filled polymers [21-26].

Pristine layered silicates usually contain hydrated Na^+ or K^+ ions [27]. Obviously, in the pristine state, layered silicates are only miscible with hydrophilic polymers, such as poly(ethylene oxide) [28], or poly(vinyl alcohol) [29]. To render layered silicates miscible with other polymer matrices, one must convert the normally hydrophilic silicate surface to an organophilic one, making the intercalation of many engineering polymers possible. Generally, this can be made by ion-exchange reactions with cationic surfactants including primary, secondary, tertiary, and quaternary alkylammonium or alkylphosphonium cations. Alkylammonium or alkylphosphonium cations in the organosilicates lower the surface energy of the inorganic host and improve the wetting characteristics of the polymer matrix, and result in a larger interlayer spacing. Additionally, the alkylammonium or alkylphosphonium cations can provide functional groups that can react with the polymer matrix, or in some cases initiate the polymerization of monomers to improve the strength of the interface between the inorganic and the polymer matrix [30, 31].

Traditional structural characterization to determine the orientation and arrangement of the alkyl chain was performed using Wide Angle XRD (WAXD). Depending on the packing density, temperature and alkyl chain length, the chains were thought to lie either parallel to the silicate layers forming mono or bilayers, or radiate away from the silicate layers forming mono or bimolecular arrangements (Figure 1.3) [32]. However, these idealized structures have been shown to be unrealistic by Vaia *et al.* [33] using Fourier Transform Infrared Spectroscopy (FTIR) experiments. They showed that alkyl chains can vary from liquid-like to solid-like, with the liquid-like structure dominating as the

interlayer density or chain length decreases (Figure 1.4.), or as the temperature increases. This occurs because of the relatively small energy differences between the trans and gauche conformers; the idealized models described earlier assume all trans conformations. In addition, for longer chain length surfactants, the surfactants in the layered silicate can show thermal transition akin to melting or liquid-crystalline to liquid-like transitions upon heating.

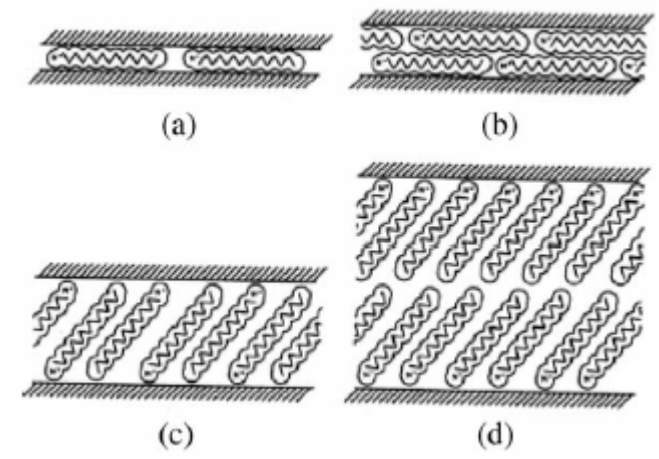

Figure 1.3. Arrangements of alkylammonium ions in mica-type layered silicates with different layer charges. Hatch areas are silicate layers [32]

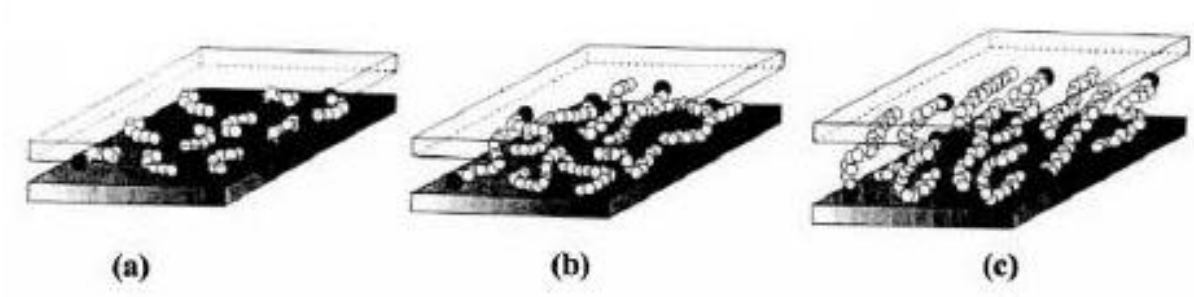

Figure 1.4. Alkyl chain aggregation models: (a) short chain lengths, the molecules are effectively isolated from each other, (b) medium lengths, quasi-discrete layers form with various degree of in plane disorder and interdigitation between the layers and (c) long lengths, interlayer order increases leading to a liquid-crystalline polymer environment. Open circles represent the CH_2 segments while cationic head groups are represented by filled circles [33]

1.1.3. Types of Nanocomposites

In general, layered silicates have layer thickness on the order of 1 nm and a very high aspect ratio (*e.g.* 10–1000). A few weight percent of layered silicates that are properly dispersed throughout the polymer matrix, thus, create much higher surface area for polymer/filler interaction as compared to conventional composites. Depending on the strength of interfacial interactions between the polymer matrix and layered silicate (modified or not), three different types of PLS nanocomposites are thermodynamically achievable (Figure 1.5):

a. *Intercalated nanocomposites*: in intercalated nanocomposites, the insertion of a polymer matrix into the layered silicate structure occurs in a crystallographically regular fashion, regardless of the clay to polymer ratio. Intercalated nanocomposites are normally interlayer by a few molecular layers of polymer. Properties of the composites typically resemble those of ceramic materials.

b. *Flocculated nanocomposites*: conceptually this is same as intercalated nanocomposites. However, silicate layers are some times flocculated due to hydroxylated edge–edge interaction of the silicate layers.

c. *Exfoliated nanocomposites*: in an exfoliated nanocomposite, the individual clay layers are separated in a continuous polymer matrix by an average distances that depends on clay loading. Usually, the clay content of an exfoliated nanocomposite is much lower than that of an intercalated nanocomposite.

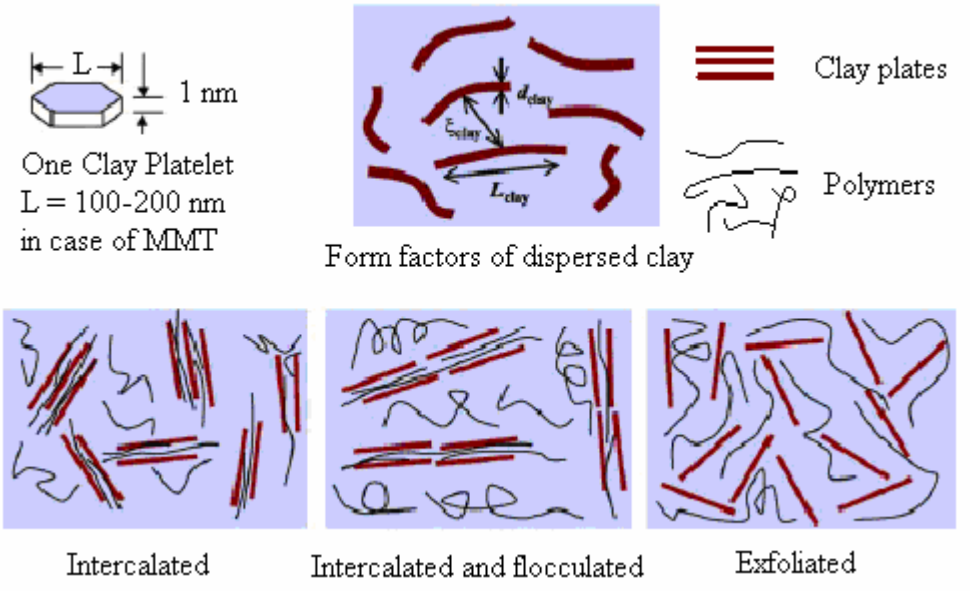

Figure 1.5. Schematically illustration of three different types of thermodynamically achievable PLS nanocomposites [34]

1.1.4. Polymers Used in Nanocomposite Syntheses

Great number of different polymers have already been used to synthesize polymer-clay nanocomposites. Polyamide-6 is the first and the most studied thermoplastic for the syntheses of polymer-clay nanocomposites [35-36]. Polyamide 6-clay hybrids were first discovered by Toyota researchers in the early nineties [37].

Other thermoplastics such as poly(ethylene oxide) [38], poly(methyl methacrylate) [39], poly(butadiene-acrylonitrile) [40], poly(ε-caprolactone) [41], polystyrene [42-43], polyimide [44-45] and poly(ethylene terephthalate) [46] have been used to synthesize polymer-clay nanocomposites by different methods. Polypropylene-clay nanocomposites have also been actively studied by the researchers from Toyota [47-50]. They used a maleic anhydride-modified polypropylene oligomer to delaminate the clay in the polypropylene matrix. The maleic anhydride gives a sufficient polarity to the modified polypropylene in order to obtain an intercalated nanocomposite.

Thermoset polymers have also been used to obtain polymer nanocomposites. Epoxy-clay nanocomposites have been extensively studied [51-53]. The reason for this is that the reactants of epoxy systems have a suitable polarity in order to diffuse between the

clay layer and form a delaminated nanocomposite upon polymerization. In the literature, nanocomposites based on polyurethanes [53-55] and silicone rubbers [56-57] have also been reported.

1.1.5. Preperation Methods of Polymer-Clay Nanocomposites

1.1.5.1. Intercalation of Polymer or Pre-polymer from Solution. This method can be used when the polymer or pre-polymer is soluble and the silicate layers are swellable. In this method, the layered silicate is first swelled in a solvent, such as water, chloroform, or toluene. When the polymer and layered silicate solutions are mixed, the polymer chains intercalate and displace the solvent within the interlayer of the silicate. Upon solvent removal, the intercalated structure remains, resulting in PLS nanocomposite.

The thermodynamics involved in this method are described in the following. For the overall process, in which polymer is exchanged with the previously intercalated solvent in the gallery, a negative variation in the change in Gibbs Free Energy (ΔG) is required. The driving force for the polymer intercalation into layered silicate from solution is the entropy gained by desorption of solvent molecules, which compensates for the decreased entropy of the confined, intercalated chains [60]. Using this method, intercalation only occurs for certain polymer/solvent pairs. This method is good for the intercalation of polymers with little or no polarity into layered structures, and facilitates production of thin films with polymer-oriented clay intercalated layers. However, from commercial point of view, this method involves the copious use of organic solvents, which is usually environmentally unfriendly and economically prohibitive.

Water-soluble polymers, such as poly(ethylene oxide) [28], poly(vinylalcohol) [29], poly(vinylpyrrolidone) [61], and poly(ethylenevinylacetate) [62], have been intercalated into the clay galleries using this method. Examples from non-aqueous solvents are nanocomposites of poly(caprolactone)/clay [63] and Poly(L-lactide)/clay [64] in chloroform as a co-solvent, and high-density polyethylene with xylene and benzonitrile [65]. Nematic liquid crystal PLS nanocomposites have also been prepared using this method in various organic solvents, such as toluene and dimethylformamide [66].

1.1.5.2. In-situ Intercalative Polymerization Method. In this method, to let the polymers form between the intercalated sheets, the layered silicate is swelled within the liquid monomer or a monomer solution. Polymerization can be initiated either by heat or radiation, by the diffusion of a suitable initiator, or by an organic initiator or catalyst fixed through cation exchange inside the interlayer before the swelling step.

According to Messersmith and Giannelis [53] (Figure 1.6), the driving force of the "in-situ polymerization" method is linked to the polarity of the monomer molecules and is believed that during the swelling phase, the high surface energy of the clay attracts polar monomer molecules so that they diffuse between the clay layers. When a certain equilibrium is reached the diffusion stops and the clay is swelled in the monomer to a certain extent corresponding to a perpendicular orientation of the alkylammonium ions. When the polymerization is initiated, the monomer starts to react with the curing agent. This reaction lowers the overall polarity of the intercalated molecules and displaces the thermodynamic equilibrium so that more polar molecules are driven between the clay layers. As this mechanism occurs, the organic molecules can delaminate the clay. Polymer-clay nanocomposites based on epoxy [58], polyurethanes [54, 55] and polyethylene terephthalate [59] have been synthesized by this method.

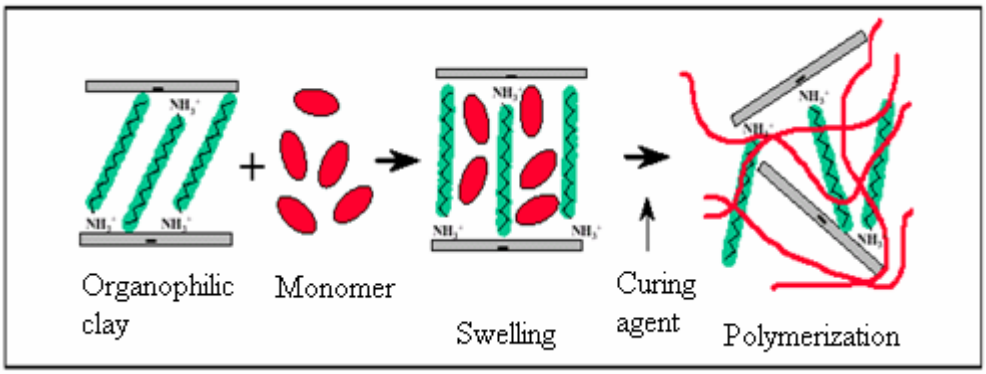

Figure 1.6. The in-situ intercalative polymerization technique [53]

1.1.5.3. Melt Intercalation. It was the year of 1993, when the melt intercalation process was first reported by Vaia *et al*. [42]. In this method, the layered silicate is mixed with the polymer matrix in the molten state. The mixture is then annealed at a temperature above the glass transition temperature of the polymer and forms a nanocomposite. In this technique no solvent is required. Under these conditions and if the layer surfaces are sufficiently compatible with the chosen polymer, the polymer can diffuse into the interlayer space and form either an intercalated or an exfoliated nanocomposite [67]. Conformational entropy of the polymer chains are lost during the intercalation. The proposed driving force for this mechanism is the important enthalpic contribution of the polymer/organoclay interactions during the blending and annealing steps. Many polymer/organosilicate hybrids obtained by melt intercalation have been investigated in recent years. A wide range of thermoplastics, from strongly polar polyamide-6 [68] to polystyrene [69] have been intercalated between clay layers by this method.

1.1.6. Techniques Used for the Characterization of Nanocomposites

The two techniques that have been mainly used for the characterization of nanocomposites are TEM and WAXD.

TEM is an imaging technique whereby a beam of electrons is focused onto a specimen causing an enlarged version to appear on a fluorescent screen or layer of photographic film, or to be detected by a Charge Coupled Device (CCD) camera.

Due to its easiness and availability WAXD is most commonly used to probe the nanocomposite structure. By monitoring the position, shape, and intensity of the basal reflections from the distributed silicate layers, the nanocomposite structure (intercalated or exfoliated) may be identified. For example, in an exfoliated nanocomposite, the extensive layer separation associated with the delamination of the original silicate layers in the polymer matrix results in the eventual disappearance of any coherent XRD from the distributed silicate layers. On the other hand, for intercalated nanocomposites, the finite layer expansion associated with the polymer intercalation results in the appearance of a new basal reflection.

Moreover, TEM allows a qualitative understanding of the internal structure, spatial distribution of the various phases, and views of the defect structure through direct visualization of polymers for the preparation of nanocomposites.

The WAXD patterns and corresponding TEM images of three different types of nanocomposites are presented in Figure 1.7. Lighter background belongs to the polymer matrix and the darker areas correspond to the silicate platelets.

WAXD is mainly used to identify intercalated structure. Usually, the intercalation of the polymer chains increases the interlayer spacing of the clay. This increase leads to a shift of a diffraction peak through lower angle values. As there is no order between clay layers in the exfoliated structure, no more diffraction peaks are visible in the XRD patterns.

Both TEM and WAXD are essential tools [70] for evaluating nanocomposite structures. However, TEM is time-intensive, and only gives qualitative information on the sample as a whole, while the low-angle peaks in WAXD allow quantification of changes in layer spacing. Generally, the structure of nanocomposites has typically been established using WAXD analyses and TEM. Typically, when layer spacing exceeds 6–7 nm in intercalated nanocomposites or when the layers become relatively disordered in exfoliated nanocomposites, associated WAXD features weaken to the point of not being useful. In this case, TEM is an essential method to prove the exfoliated structure of the nanocomposite as it gives a picture of the structure.

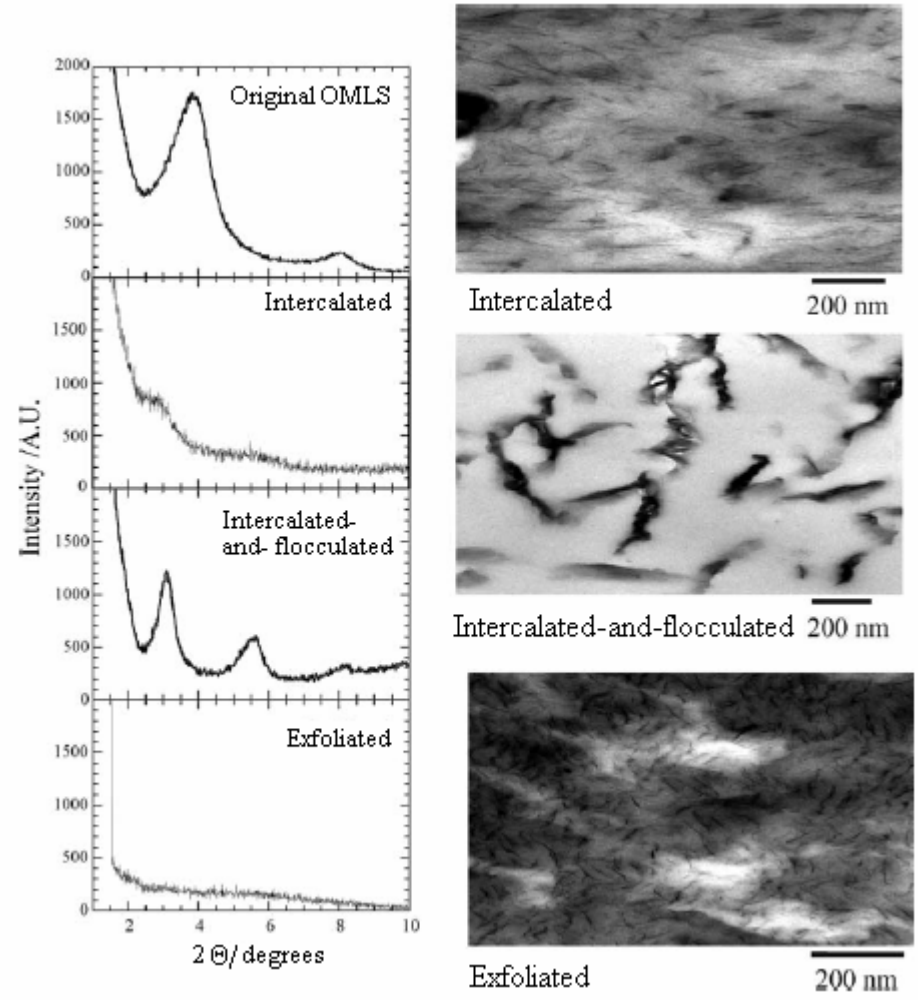

Figure 1.7. (a) WAXD patterns and (b) TEM images of three different types of nanocomposites [6]

1.1.7. Nanocomposite Properties

Nanocomposites consisting of a polymer and layered silicate (modified or not) frequently exhibit remarkably improved mechanical and materials properties when compared to those of pristine polymers containing a small amount (≤ 5 weight %) of layered silicate. Improvements include a higher modulus which means higher stiffness, increased strength and heat resistance, decreased gas permeability and flammability and increased biodegradability of biodegradable polymers. The main reason for these improved properties in nanocomposites is the stronger interfacial interaction between the matrix and layered silicate, compared with conventional filler-reinforced systems.

1.2. Photoinitiated Polymerization

In radical photopolymerization, polymerizations are initiated by light and both the initiating species and the growing chain ends are radicals. As for other polymerizations, molecules of appreciably high molecular weight can be formed in the course of the chain reaction. Playing the predominant role in technical polymer syntheses, vinyl monomers can be mostly polymerized by a radical mechanism. Exceptions are vinyl ethers, which have to be polymerized in an ionic mode [71,72].

Regarding the initiation by light, it has to be pointed out that the absorption of incident light by one or several components of the polymerization mixture, is a crucial prerequisite. If the photon energy is absorbed directly by a photosensitive compound, being the monomer itself or an added initiator, the photosensitive substance undergoes a homolytic bond rapture forming radicals, which may initiate the polymerization. In some cases, however, the photon energy is absorbed by a compound that itself is not prone to radical formation. These so called sensitizers transfer their electronic excitation energy to reactive constituents of the polymerization mixture, which finally generate radicals. The radicals evolved will react with intact vinyl monomer starting a chain polymerization. Under favorable conditions, a single free radical can initiate the polymerization of a thousand molecules. The spatial distribution of initiating species may be arranged in any desired manner.

Light induced free radical polymerization is of enormous commercial use. Techniques such as curing of coatings on wood, metal and paper, adhesives, printing inks and photoresists are based on photoinitiated radical vinyl polymerization. There are some other interesting applications including production of laser video discs and curing of acrylate dental fillings.

In contrast to thermally initiated polymerizations, photopolymerization can be performed at room temperature. This is a striking advantage for both classical polymerization of monofunctional monomers and modern curing applications. Photopolymerization of monofunctional monomers takes place without side reactions such as chain transfer. In thermal polymerization, the probability of chain transfer is high which brings about a high amount of branched macromolecules. Hence, low-energy stereospecific

polymeric species, namely of syndiotactic configuration, may be obtained by photopolymerization. Another important use refers to monomers with low ceiling temperature. They can only be polymerized at moderate temperatures, otherwise depolymerization dominates over polymerization. By means of photopolymerization these monomers are often easily polymerizable. Furthermore, biochemical applications, such as immobilization of enzymes by polymerization, do also usually require low temperatures. As far as curing of coatings or surfaces is concerned it has to be noted, that thermal initiation is often not practical, especially if large areas or fine structures are to be cured or if the curing formulation is, like for dental fillings, placed in a surrounding that should rather not be heated.

Radical photopolymerization of vinyl monomers played an important role in the early development of polymerization. One of the first procedures for polymerizing vinyl monomers was the exposure of monomer to sunlight. Blyth and Hoffman [73] reported on the polymerization of styrene by sunlight more than 150 years ago.

Photocurable formulations are mostly free of additional organic solvents; the monomer, which serves as reactive diluent, is converted to solid, environmentally safe resin without any air pollution. Ultraviolet (UV) curing is often a very fast process, taking place as pointed out above without heating. If the polymerization mixture absorbs solar light and the efficiency of radical formation is high, photocuring can be performed with no light source but sun light. These features make photopolymerization an ecologically friendly and economical technology that has high potential for further development.

1.2.1. Photoinitiated Free Radical Polymerization

Photoinitiated free radical polymerization consists of photoinitiation, propagation, chain transfer and termination;

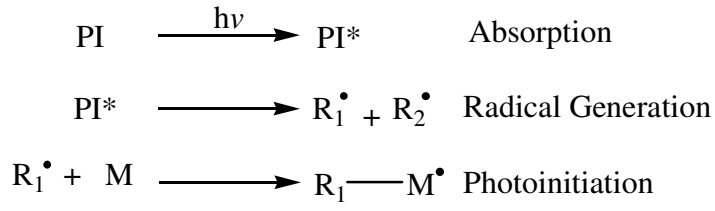

The role that light plays in photopolymerization is restricted to the very first step, namely the absorption and generation of initiating radicals. The reaction of these radicals with monomer, propagation, transfer and termination are purely thermal processes; they are not affected by light.

Photoinitiation involves absorption of light by a photosensitive compound or transfer of electronic excitation energy from a light absorbing sensitizer to the photosensitive compound. Homolytic bond rupture leads to the formation of a radical that reacts with one monomer unit. Repeated addition of monomer units to the chain radical produces the polymer backbone (propagation).

Chain transfer also takes place, that is, growing chains are terminated by hydrogen abstraction from various species (*e.g.,* from solvent) and new radicals capable of initiating other chain reactions are formed.

Finally, chain radicals are consumed by disproportionation or recombination reactions. Termination can also occur by recombination or disproportionation with any other radical included primary radicals produced by photoreaction.

1.2.2. Absorption of Light

The absorption of light excites the electrons of a molecule, what lessens the stability of a bond, and can, under favorable circumstances, lead to its dissociation. Functional groups that have high absorbency, like phenyl rings or carbonyl groups, are referred to as chromophoric groups. Naturally, photoinduced bond dissociations do often take place in the proximity of the light absorbing chromophoric groups. In some examples, however, electronic excitation energy may be transferred intramolecularly to fairly distant, but easily cleavable bonds to cause their rupture.

The intensity I_a of radiation absorbed by the system is governed by the Beer Lambert law;

$$I_a = I_0 (1 - e^{-\acute{\varepsilon} 1 [S]})$$

where I_0 is the intensity of light falling on the system, l is the optical path length and [S] is the concentration of the absorbing molecule having the molar extinction coefficient, ε.

If the monomer possesses chromophoric groups and if it is sensitive towards light (*i.e.*, it undergoes photoinduced chemical reactions with high quantum yields) one can carry out photopolymerizations by just irradiating the monomer. In many cases, however, monomers are not efficiently decomposed into radicals upon irradiation. Furthermore, monomers are often transparent to light at $\lambda \geq 320$ nm, where commercial lamps emit. In these cases, photoinitiators are used. These compounds absorb light and bring about the generation of initiating radicals.

1.2.3. Radical Generation

1.2.3.1. Radicals *via* Monomer Irradiation. In some cases, a monomer may function as a photoinitiator and become incorporated into a copolymer chain. This has been shown for styrene and other conjugated monomers when exposed to deep-UV light; however, the initiation efficiency in these systems is substantially less than when a photoinitiator is present. A better polymerizable initiator scheme is illustrated by the acceptor-donor chemistry of maleimide-donor systems [74]. Maleimide acts as both photoinitiator and comonomer in the presence of hydrogen donors such as vinyl ethers or vinyl esters [75,76]; an example of this copolymerization is shown below.

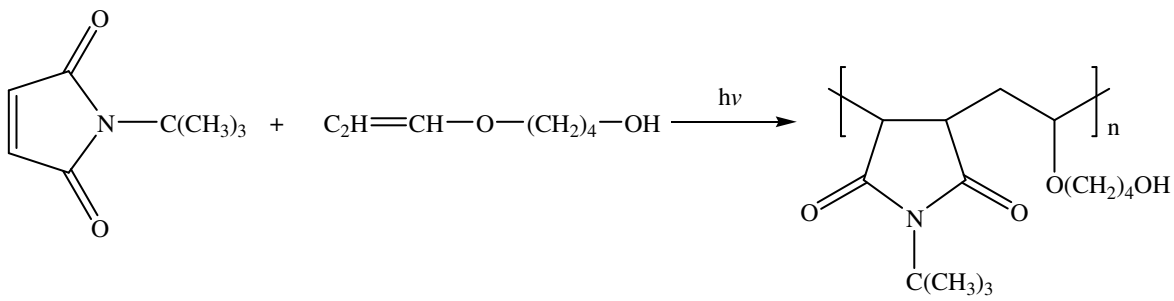

It shows the molecular structure of the acceptor tert-butylmaleimide (left), the donor 4-hydroxy-butyl vinyl ether (right), and their corresponding copolymer repeating unit [77].

Readily available monomers, which to some extent undergo polymerization and copolymerization upon UV irradiation, are as follows: allyl methacrylate, barium acrylate, cinnamyl methacrylate, diallyl phthalate, diallyl isophtalate, diallyl terephthalate, 2-ethylhexyl acrylate, 2-hydroxyethyl methacrylate, 2-hydroxypropyl acrylate, styrene, methylenebisacrylamide, methyl methacrylate, pentaerythritol, tetramethacrylate, tetraethylene glycol, dimethacrylate, tetrafluoroethylene, *N*-vinylcarbazole, vinyl cinnamate, vinyl 2-fluorate and vinyl 2-fruyl acrylate [78].

1.2.3.2. Radical Generation by Initiators. In the photoinduced polymerization applications, initiators are usually used to generate radicals. Photoinitiators are generally divided into two classes according to the process by which initiating radicals are formed [79].

Compounds which undergo unimolecular bond cleavage upon irradiation are termed as type I photoinitiators or PI_1- type initiators:

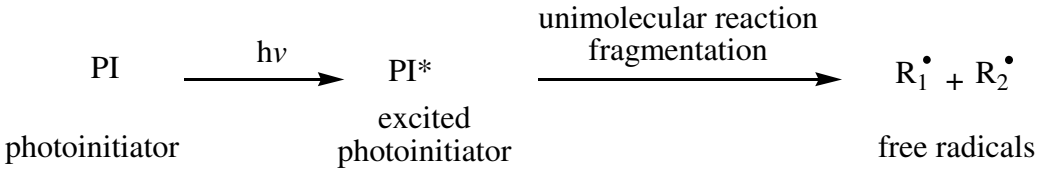

If the excited state photoinitiator interacts with a second molecule (a coinitiator (COI) to generate radicals in a bimolecular reaction, the initiating system is termed as a type II photoinitiator or PI_2-type initiator:

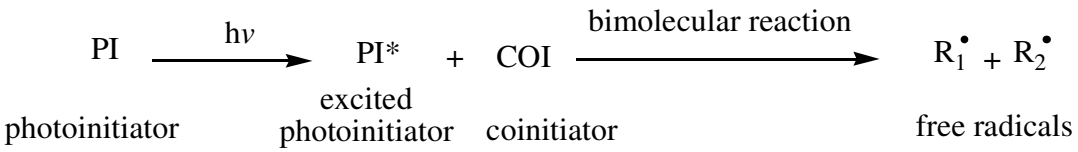

Efficient photoinitiators of both classes are known and found everyday usage. Type I photoinitiators are highly reactive UV photoinitiators, but are less frequently used in visible light curing systems. Type II photoinitiators are versatile initiators for UV curing system and visible light photoinitiators belong almost exclusively to this class of photoinitiators.

Type I Photoinitiators: *Unimolecular Photoinitiators*. These substances undergo a homolytic bond cleavage upon absorption of light;

$$PI \xrightarrow{h\nu} PI^* \longrightarrow R_1^{\bullet} + R_2^{\bullet}$$

The fragmentation that leads to the formation of radicals is, from the point of view of chemical kinetics, a unimolecular reaction;

$$\frac{d[R_1^{\bullet}]}{dt} = \frac{d[R_2^{\bullet}]}{dt} = k\ [PI^*]$$

The number of initiating radicals formed upon absorption of one photon is termed as quantum yield of radical formation ($\Phi_{R\bullet}$):

$$\Phi_{R\bullet} = \frac{\text{Number of initiating radicals formed}}{\text{Number of photons absorbed by the photoinitiator}}$$

Theoretically, cleavage type photoinitiators should have a $\Phi_{R\bullet}$ value of two since two radicals are formed by the photochemical reaction. The values observed, however, are much lower because of various deactivation routes of the photoexcited initiator other than radical generation. These routes include physical deactivation such as fluorescence or non-radiative decay and energy transfer from the excited state to other, ground state molecules, a process referred to as quenching.

The reactivity of photogenerated radicals with polymerizable monomers is also to be taken into consideration. In most initiating systems, only one in two radicals formed adds to monomer thus initiating polymerization. The other radical usually undergoes either combination or disproportionation. The initiation efficiency of photogenerated radicals (f_P) can be calculated by the following formula:

$$f_P = \frac{\text{Number of chain radicals formed}}{\text{Number of primary radicals formed}}$$

The overall photoinitiation efficiency is expressed by the quantum yield of photoinitiation (Φ_P) according to the following equation:

$$\Phi_P = \Phi_{R\bullet} \times f_P$$

Regarding the energy necessary, it has to be said that the excitation energy of the photoinitiator has to be higher than the dissociation energy of the bond to be ruptured. The bond dissociation energy, on the other hand, has to be high enough in order to ensure long term storage stability. The majority of type I photoinitiators are aromatic carbonyl compounds with appropriate substituents, which spontaneously undergo α-cleavage generating free radicals according to reaction below.

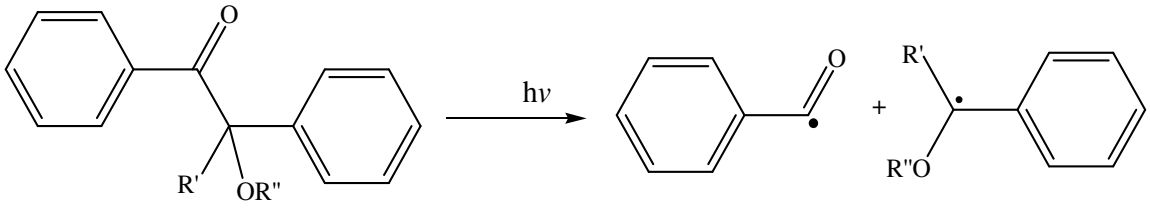

R' = H, alkyl, subst. alkyl
R" = H, alkyl, subst. alkyl

The benzoyl radical formed by the reaction depicted is very reactive towards the unsaturations of vinyl monomers [75].

The α-cleavage often referred to as Norrish type I reaction [80] of carbonyl compounds starts from the initiator's triplet state, which is populated *via* intersystem crossing. Notably, the excited triplet states are usually relatively short lived that prevents excited molecules to undergo side reactions with constituents of the polymerization mixture. While triplet quenching by oxygen can, in most cases, be neglected due to the short lifetime of the triplet states, quenching by monomer sometimes plays a role. However, this refers exclusively to monomers with low triplet energies, like styrene (E_T = 259 kJ mol^{-1} [81]).

If the absorption characteristics of a cleavable compound are not meeting the requirements, *i.e.*, the compound absorbs at too low wavelengths, the use of sensitizers (S) with matching absorption spectra is recommendable. Sensitizers absorb the incident light and are excited to their triplet state;

$$S \xrightarrow{h\nu} {}^3S^*$$

The triplet excitation energy is subsequently transferred to the photoinitiator which forms initiating radicals;

$${}^3S^* + PI \longrightarrow S + {}^3PI^*$$

This process has to be exothermic, *i.e.*, the sensitizers triplet energy has to be higher than the triplet energy level of the initiator. Through energy transfer, the initiator is excited and undergoes the same reactions of radical formation as if it were excited by direct absorption of light. The sensitizer molecules return to their ground state upon energy transfer; they are therefore not consumed in the process of initiation.

Type II Photoinitiators: *Bimolecular Photoinitiators*. The excited states of certain compounds do not undergo type I reactions because their excitation energy is not high enough for fragmentation, *i.e.*, their excitation energy is lower than the bond dissociation energy. The excited molecule can, however, react with another constituent of the polymerization mixture, the so-called COI, to produce initiating radicals;

$$PI \xrightarrow{h\nu} PI^*$$

$$PI^* + COI \xrightarrow{k} R_1^{\bullet} + R_2^{\bullet}$$

In this case, radical generation follows 2nd order kinetics;

$$\frac{d[R_1^{\bullet}]}{dt} = \frac{d[R_2^{\bullet}]}{dt} = k\ [PI^*]\ [COI]$$

There are two distinct pathways of radical generation by type II initiating systems:

(I) ***Hydrogen abstraction*** from a suitable hydrogen donor. As a typical example, the photoreduction of benzophenone by isopropanol is depicted;

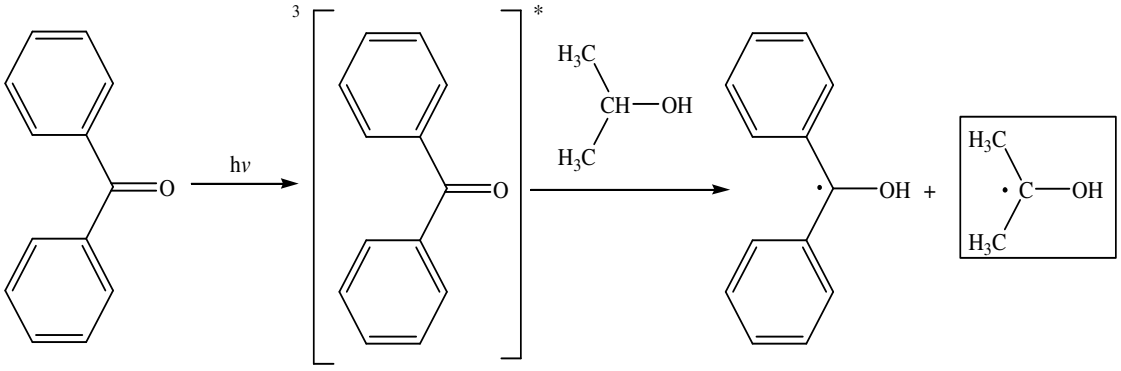

Bimolecular hydrogen abstraction is limited to diaryl ketones [82]. From the point of view of thermodynamics, hydrogen abstraction is to be expected if the diaryl ketone's triplet energy is higher than the bond dissociation energy of the hydrogen atom to be abstracted.

(II) ***Photoinduced electron transfer reactions*** and subsequent fragmentation. In electron transfer reactions, the photoexcited molecule, termed as sensitizer for the convenience, can act either as electron donor or electron acceptor according to the nature of the sensitizer and COI;

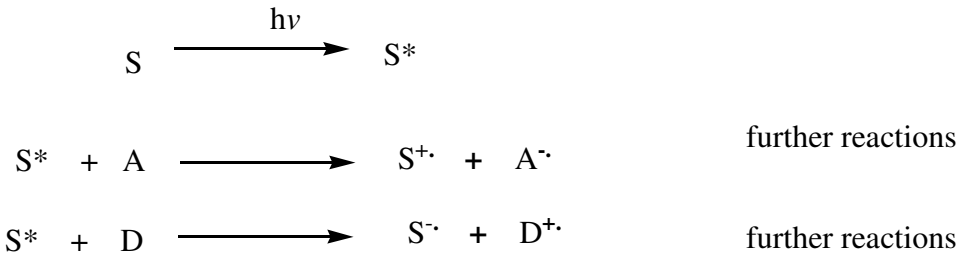

Fragmentation yields radical anions and radical cations, which are often not directly acting as initiating species themselves but undergo further reactions, by which initiating free radicals are produced.

The electron transfer is thermodynamically allowed, if ΔG calculated by the Rehm-Weller equation [83] is negative:

$$\Delta G = F [E_{1/2}^{ox} (D/D^{+\cdot}) - E_{1/2}^{red} (A/A^{-\cdot})] - E_S + \Delta e_C$$

F = Faraday constant

$E_{1/2}^{ox} (D/D^{+\cdot})$ and $E_{1/2}^{red} (A/A^{-\cdot})$ are oxidation and reduction potential of donor and acceptor, respectively

E_S = Singlet state energy of the sensitizer

Δe_C = Coulombic stabilization energy

Electron transfer is often observed for aromatic ketone/amine pairs and always with dye/COI systems.

1.3. Photoinduced Polymerization of MMA

PMMA is used in a variety of applications due to its optical properties. It may be prepared by a radical mechanism using thermal and photoinitiators. Radicals generated upon irradiation react with the double bond of the monomer to yield PMMA;

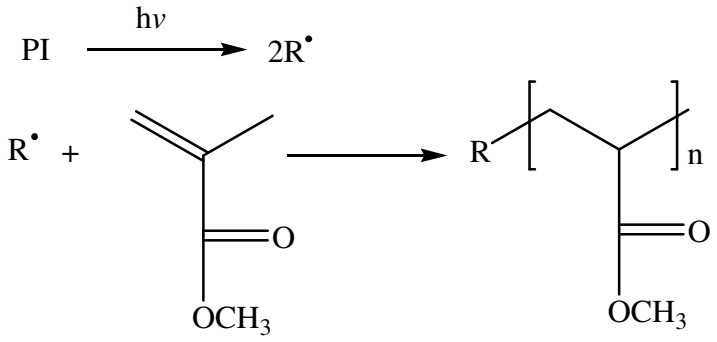

1.4. Photopolymerization Usage in Nanocomposite Preparation

Light induced polymerization has becoming a well-accepted method to prepare nanocomposites because of its unique advantages. They can be conducted at room temperature, which is an outstanding advantage for both classical polymerization of monofunctional monomers and modern curing applications. By means of photopolymerization, for instance, monomers with low ceiling temperatures can easily be polymerized without depolymerization taking place. In curing of coatings or surfaces, where thermal polymerizations are not feasible, photopolymerizations can be employed with success. Moreover, reactive sites can be generated at definite positions in the macromolecule, owing to the selective absorptivity of certain chromophoric groups located accordingly. However, photopolymerization has been scarcely applied to the preparation of polymer-layered clay nanocomposites.

Jui-Ming Yeh *et al.* prepared nanocomposite by using acrylamide as a monomer-intercalating agent [84]. They first intercalated organic acrylamide monomers into the interlayer regions of acrylamide-treated organophilic clay hosts, and this is fallowed by one step ultraviolet radiation polymerization with benzil which is used as a photoinitiator. They also investigated the effect of different loading degrees. The effects of the material composition on the thermal stability, optical clarity and gas barrier properties were also studied by them.

In another study [85], Huimin *et al.* used an independent low-molar mass compound such as octadecyl amine as an intercalenting agent. They prepared

polymer/MMT intercalation composite materials by two kinds of photo-polymerization reaction (photo-acid generation and photo-radical generation). Small angle XRD was used for the structural characterization of MMT contained in the products. They resulted that, after chemical modification of MMT, the monomer (MMA) and the prepolymer (m-cresol/ hexamethoxymethylmelamine) were able to intercalate into the layers of clay and to polymerize "in situ", thus producing photo-polymerized composite materials.

Uhl *et al*. [86] reinforced UV curable films with an organically modified MMT. They preperad organically modified MMTs by an ion exchange process, in which sodium ions were replaced by alkyl ammonium ions. In this process, they first suspended MMT in distilled water followed by addition of organo-ammonium salt. Then they washed organically modified MMT until no anion could be detected in a silver nitrate solution. Cetyltrimethylammonium bromide MCs gave rise to better intercalated clay morphology. They characterized the microstructures by XRD and TEM. Physical properties were examined by Real Time Infrared Spectroscopy (RTIR), DSC, photo-DSC, Dynamic Mechanical Analyses (DMA). Some tensile properties were also reported. They noted that thermal and mechanical properties were generally improved with nanoclay reinforcements. The effects of nanoclays on the properties of UV-curable films are critically evaluated in this paper reported a moderate enhancement of some of the properties of UV-cured acrylate films containing layered silicates as nanomaterial.

Christian Decker and his group successfully used the UV-curing technology to produce rapidly a polyacrylate/clay nanocomposite at room temperature [87-88]. They made clay organophilic by a treatment with hexadecyl trimethylammonium chloride. The addition of the mineral filler did not affect significantly the polymerization kintetics in thin films (30 μm), at clay concentrations up to 7 weight %. This method of producing polymer nanocomposites has been extended to different types of UV-curable resins (epoxides, vinyl ethers, hybrids) [89], as well as to other systems [90-92].

Very recently, Jianbo Di and Dotsevi Y. Sogah [92] reported that they achieved living radical polymerization by using a silicate-anchhored photoiniferter as an intercalating agent to prepare nanocomposites. Thus, nanocomposites containing polystyrene, poly(methlymethacrylate), poly(tert-butylmethacrylate) and poly(methyl

methacrylate-b-styrene) of controlled molecular weight, architecture and polydispersity were prepared. They could reach to the exfoliation level even with very high degrees of MMT loading as all polymer chains are ionically bonded to the clay layers.

By searching the literature, it was seen that using a photoinitiator intercalent for the syntheses of polymer-clay nanocomposites had never been tried before. This was the motivation for investigating the usage of a special salt, PDA which was expected to act as both intercalent and photoinitiator in the PMMA nanocomposite syntheses.

2. EXPERIMENTAL

2.1. Materials

N,N-dimethylaniline (98 %, Fluka) was distilled prior to use. Bromoacetophenone (Fluka), potassiumhexafluorophosphate (Aldrich), acetone (Merck) and methanol (Merck) were used as received. MMA (≥99 %, Fluka) was distilled over CaH_2 in vacuo. MMT was kindly donated by Süd Chemie (Nanofil 1080, cationic (Na^+) exchange capacity of 100 meq./100 g).

2.2. Syntheses of PDA

Into a 100 ml round bottom flask equipped with a magnetic stirrer and a reflux condenser, 1.50 g (7.54×10^{-3} mol) of bromoacetophenone, 0.91g (7.54×10^{-3} mol) N,N-dimethylaniline and 1.39 g (7.54×10^{-3} mol) KPF_6 and 50 ml of acetone were placed. The reaction mixture was brought to reflux and held at this temperature for 15 min. The dark pink solution was filtered to remove KBr, which was formed during the reaction. Then the solvent was removed on a rotary evaporator, leaving PDA as a tan solid. The product was recrystallized twice from methanol solution. The salt washed with water and dried at vacuum (mp. 118 ^oC, yield 59 %) [93].

2.3. Modification of MMT with PDA

Modification of MMT clay with PDA having quarternized ammonium ion was achieved using through ion exchange reaction. MMT (0.5 g) was dispersed in 100 ml deionized water at 50 °C and a separate solution of 0.5 g of PDA in 100 ml deionized water was heated and mixed at 50 °C for 24 hours. Then two solutions were mixed vigorously while keeping the temperature of the solution at 50 °C. After mixing, the total volume is brought up to 1800 ml and stirred for 24 hours. The MC was recovered by filtering the solution followed by repeated washings of the filter cake with deionized water to remove excess ions. The final product was dried in a vacuum oven at room temperature for 12 hours.

2.4. Preparation of the PMMA Nanocomposites by Photopolymerization

The MC (1 %, 3 %, and 5 % by weight of monomer) was mixed with MMA monomer in pyrex tubes at room temperature for 12 hours in dark. For the mixture of 1 % MC, 0.0456 g MC and 4.80 mg MMA were mixed by using magnetic stirrer. Then the mixture was degassed with nitrogen. The tube which contains the mixture was placed at the hearth of a Merry-go-round type reactor given in Figure 2.1.

There are 16 Philips 8W/06 lamps at the iner side of the reactor which are emitting light at $\lambda > 300$ nm and a cooling system which also a magnetic stirrer stands at the bottom so the mixture is stirred when it is irradiated. After 2.5 hours, viscosity increased to a level to stop the rotation of magnetic stirrer. At the end of 5 hours, polymer was removed and was precipitated into methanol, then it was filtered, dried and weighed.

Figure 2.1. Merry-go-round type reactor

2.5. Characterization

In order to measure the basal spacing (d_{001} reflection) of MMT clays, WAXD measurements were conducted on a Rigaku D/Max-Ultimat diffractometer with CuK_α radiation (λ = 1.54 Å), operating at 40 kV and 40 mA. TGA was performed on TA

Instruments (TGA/IR Interface) under nitrogen flow with a heating rate of 10 °C/min. Rheometric Scientific DSC was used under nitrogen atmosphere with a heating rate of 5 °C/min to measure T_g of the nanocomposites. Version V5.42 is used to take the DSC graphs. Fracture surfaces of the composites were investigated by SEM analyses using Philips Field-Emission Environmental Scanning Electron Microscope (ESEM-FEG) with Energy Dispersive Analyses of X-Ray (EDAX) attachment. Bright field TEM images were obtained at 100 kV, at low-dose conditions, with a JEOL/JEM-1011 electron microscope. Very thin films were cast from solution of nanocomposite in dichloromethane on carbon-coated (type B) copper grids of 200 mesh. The contrast between the silicates and the polymer phase was sufficient for imaging; therefore, no heavy metal staining of sections prior to imaging was required.

3. RESULTS AND DISCUSSIONS

3.1. Syntheses and Characterization of Intercalent-photoinitiator, PDA

PDA was synthesized by using bromoacetophenone and N,N-dimethylaniline in the presence of potassiumhexafluorophosphate [93];

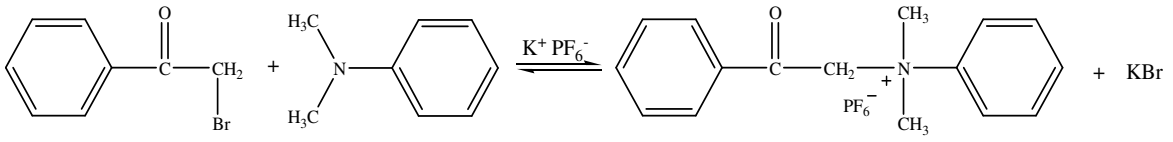

PDA is a querternary ammonium salt which may be used as an intercalant in further nanocomposite preparation studies.

The structure was confirmed by Proton Nuclear Magnetic Resonance Spectroscopy (^{1}H-NMR) spectrum given in Figure 3.1. The peaks from 7.50 ppm to 8.00 ppm belong to the aromatic hydrogens and typical for the phenyl group. The peak at 6.12 ppm belongs to the hydrogens of N^+-CH_2- and the most intense peak which is at 3.77 ppm is the proof of N^+-$(CH_3)_2$ in the structure.

Simple anilinium salts are photochemically stable. Therefore, on using these compounds no polymerization takes place upon photolysis. However, incorporation of chromophoric phenacyl moiety introduces photochemical activity to the salt. As can be seen from Figure 3.2 (a), the absorption spectrum of PDA, exhibits an n-л* at a maximum at about 300 nm, characteristic of acetophenone derivatives. This n-л* transition makes PDA useful as a photoinitiator. After 15 minutes of irradiation, the PDA undergoes an irreversible photolysis leading to fragmentation of the photoinitiator. Figure 3.2 (b) shows the absorption spectrum of fragmentation products of PDA. It is also clear from the graph that the wavelength reached a maximum at 255 nm.

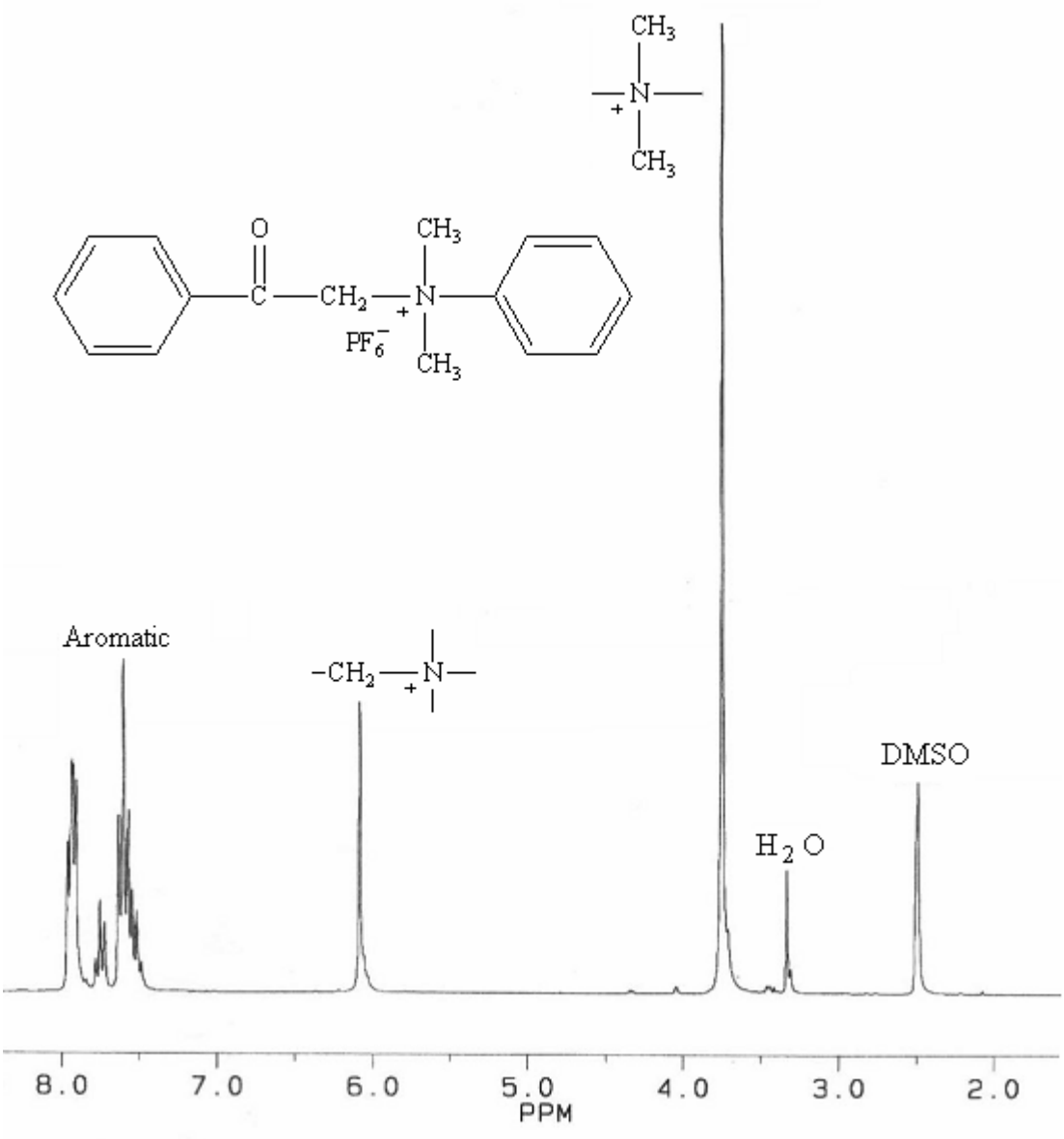

Figure 3.1. ^{1}H-NMR spectrum of PDA in DMSO [93]

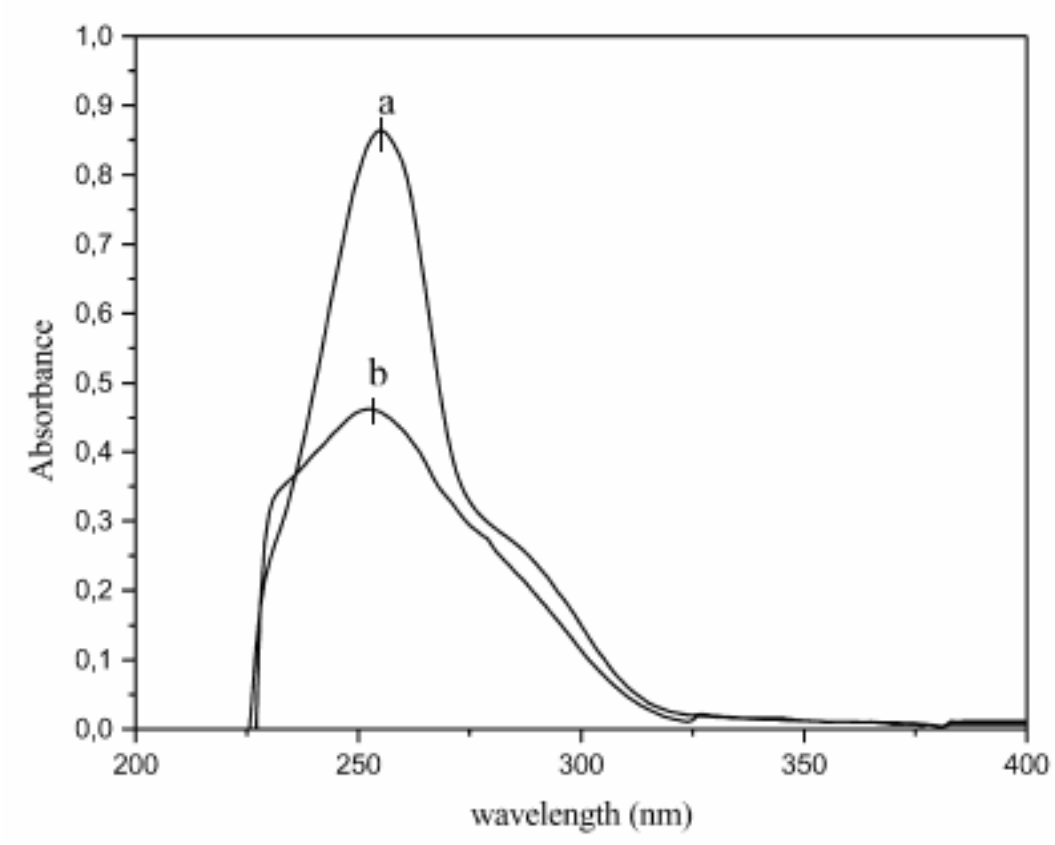

Figure 3.2 Absorption spectra of PDA in dichloromethane before (a) and after 15 minutes of irradiation (b) [93]

3.2 Modification of Na-MMT with PDA

MMT is a natural and hydrophilic clay. In order to be compatible with organic polymers, its organophilicity has to be improved. MMTs have been treated with mostly quaternary ammonium salts to obtain organophilic clay. Quaternary ammonium salts can be easily exchanged with the hydrated cations between the silicate layers resulting in increase in the spacing between the clay layers [31].

PDA possesses ammonium cations in the structure and they can readily be exchanged with the ions in the silicate layers (Figure 3.3).

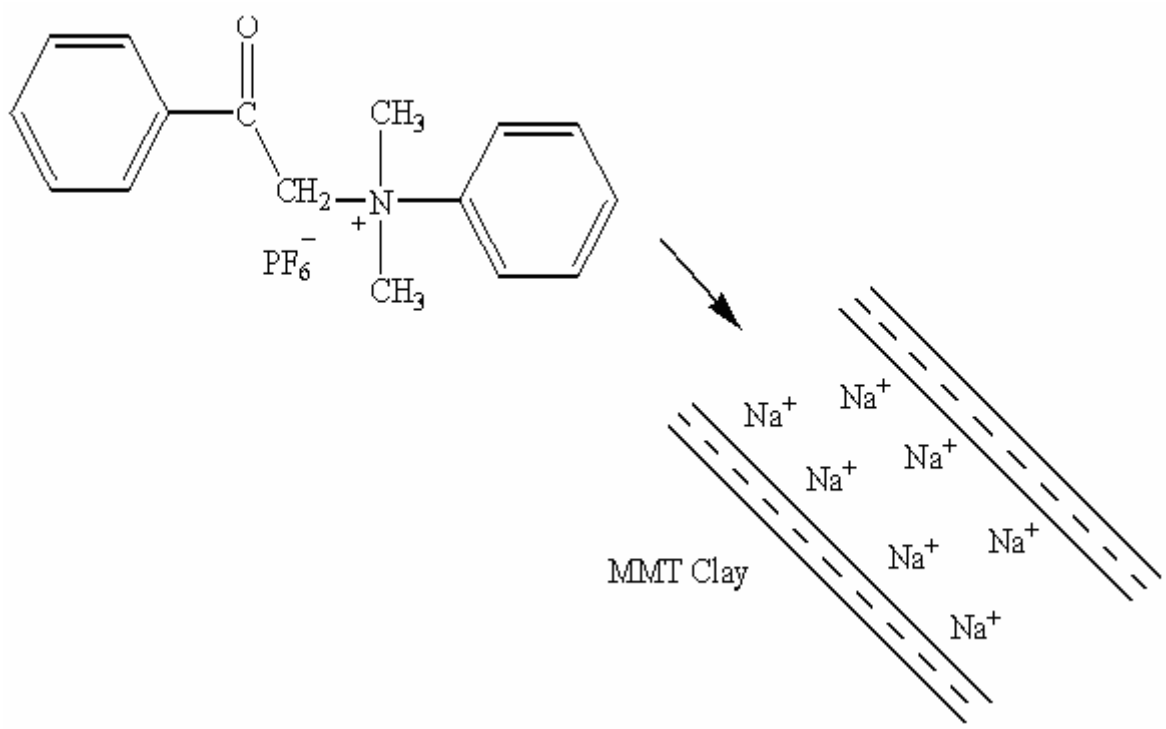

Figure 3.3. Modification of Na-MMT with PDA

Na-MMT with a cation exchange capacity of 100 meq./100 g was modified by PDA. In order to verify the intercelation, MC was then characterized by XRD analyses. Figure 3.4 shows that basal spacings of Na-MMT and MC which were obtained from the peak position of the d_{001} reflection in the XRD patterns. The d-spacings of Na-MMT and MC were found to be 12.13 Å and 17.11 Å, respectively. It is very well known that this increase is a proof of insertion of a greater molecule between clay layers [32]. In a similar way, increment of interlayer spacing here is an indication of successful insertion of PDA into MMT layers.

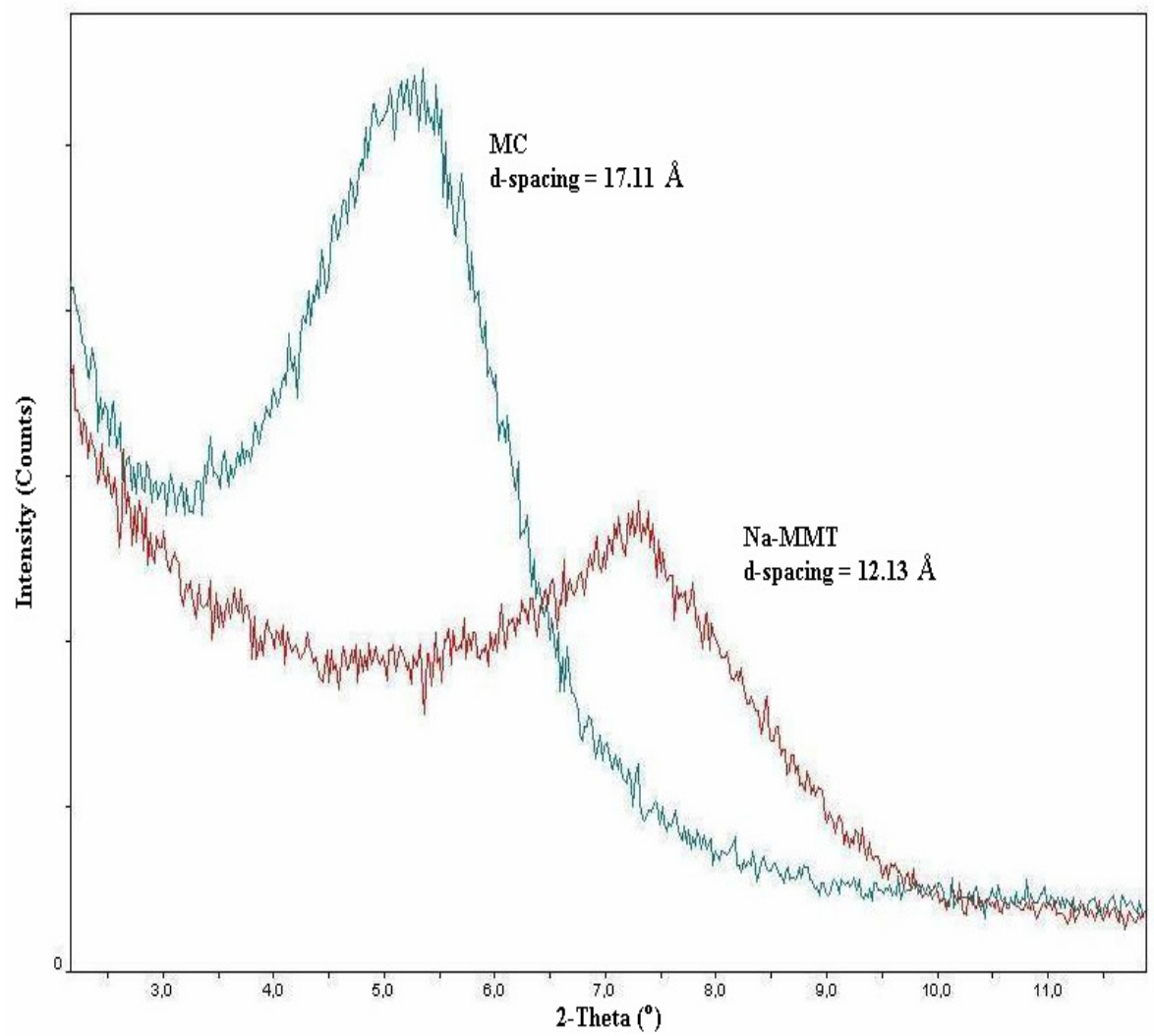

Figure 3.4. XRD patterns of Na-MMT and MC

3.3 Syntheses of PMMA Nanocomposites

It was previously shown that depending on the counter anion, PDA initiates the polymerization of appropriate monomers *via* cationic, [93, 94] zwitterionic and free radical mechanisms [95]. The following mechanism for the initiation of the free radical polymerization of MMA by PDA was suggested;

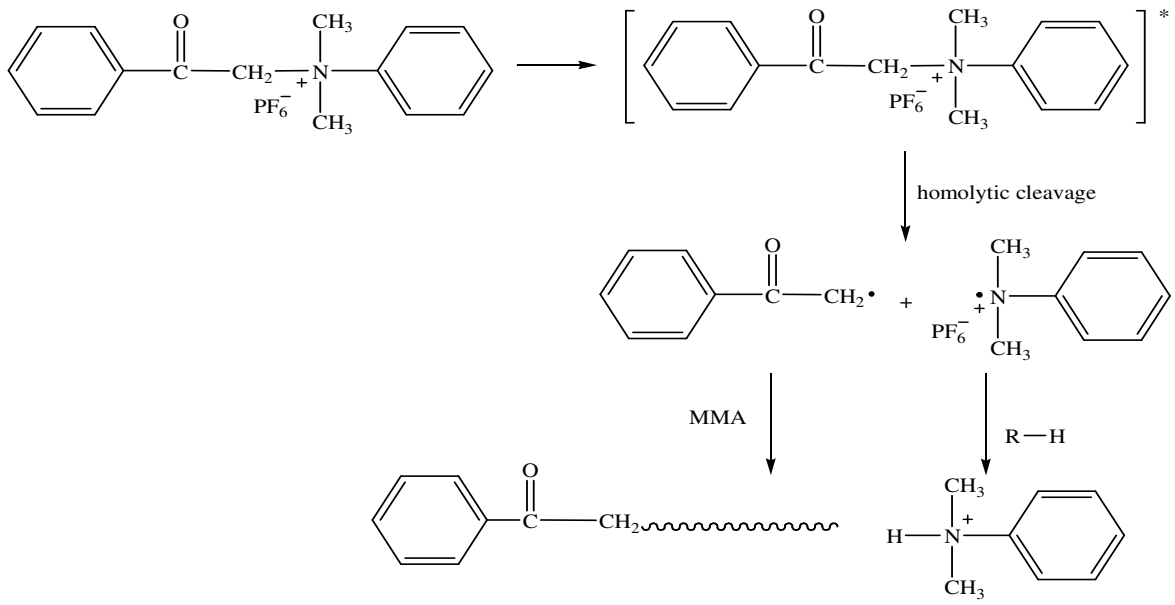

Electronically excited PDA may undergo homolytic cleavage resulting in the formation of free radicals capable of initiating polymerization of MMA. As can be seen from the reaction below, when the monomer is dispersed, the chain growth occurs in the intercalated layer.

The preperation of PMMA nanocomposites *via* in-situ photopolymerization technique is schematized in Figure 3.5.

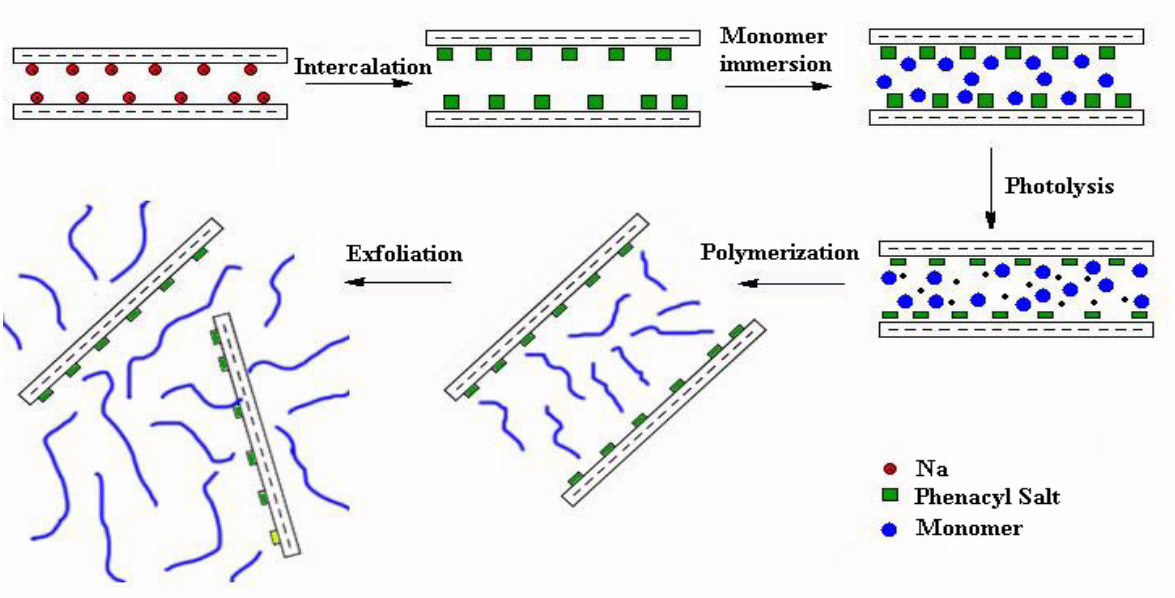

Figure 3.5 Schematic representation of clay-PMMA nanocomposites by photoinitiated radical polymerization

The resultant nanocomposite was characterized with XRD technique. Figure 3.6 gives the XRD patterns of MC, Na-MMT, PMMA-1%MC and their detailed data are summarized in Table 3.1. Nonexistence of any d_{001} reflection peak is a clear support to conclude that PMMA-1%MC shows an exfoliated structure [90].

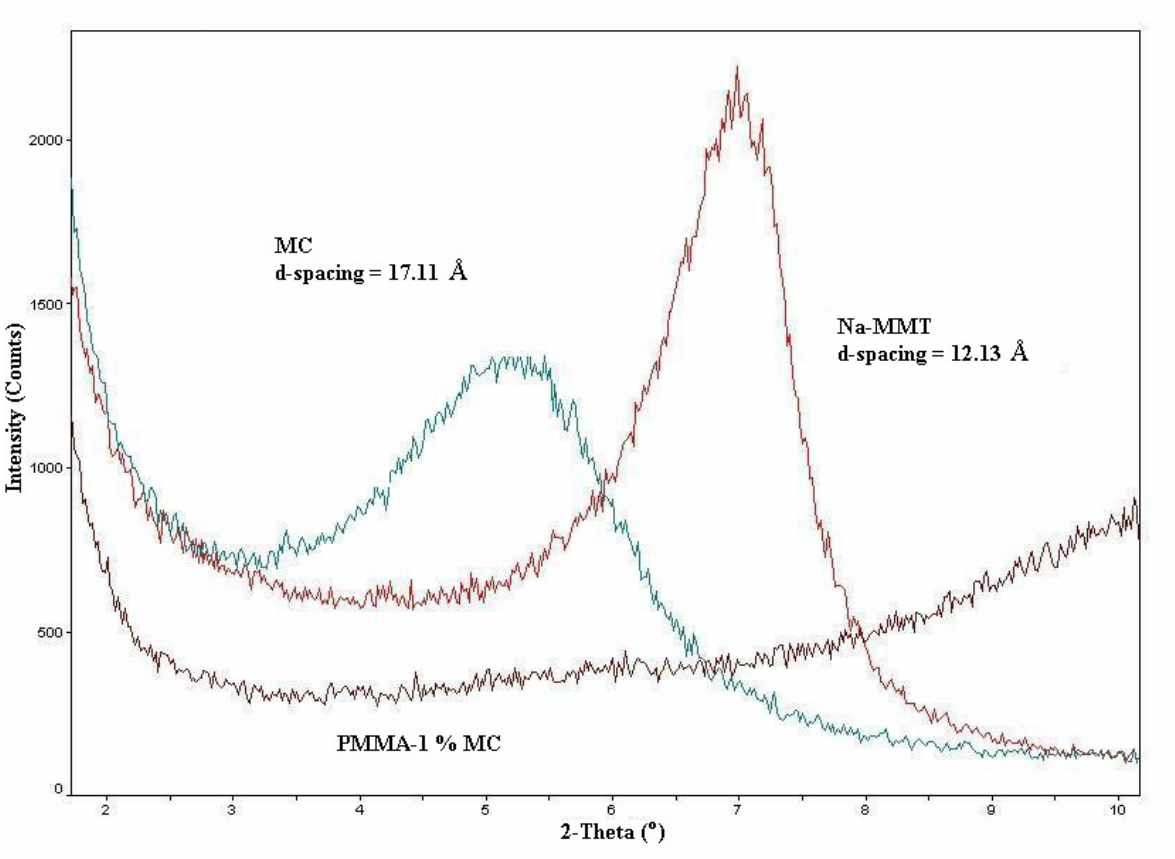

Figure 3.6 XRD patterns of Na-MMT, MC and PMMA-1%MC

Table 3.1 XRD data results for the clays used and PMMA-1%MC

Clays and nanocomposites	d_{001} of clay (Å)
NaMMT	12.13
MC	17.11
PMMA-1%MC	No reflection

TGA graphs of PMMA and PMMA-1%MC are given in Figure 3.7. It is clear that PMMA-1%MC has higher onset degradation temperature than PMMA. This improved stability in nanocomposite may be attributed to maximized interaction between the clay and the polymer in an exfoliated nanocomposite structure as this increases the surface area of clay which is covered by polymer matrix [30].

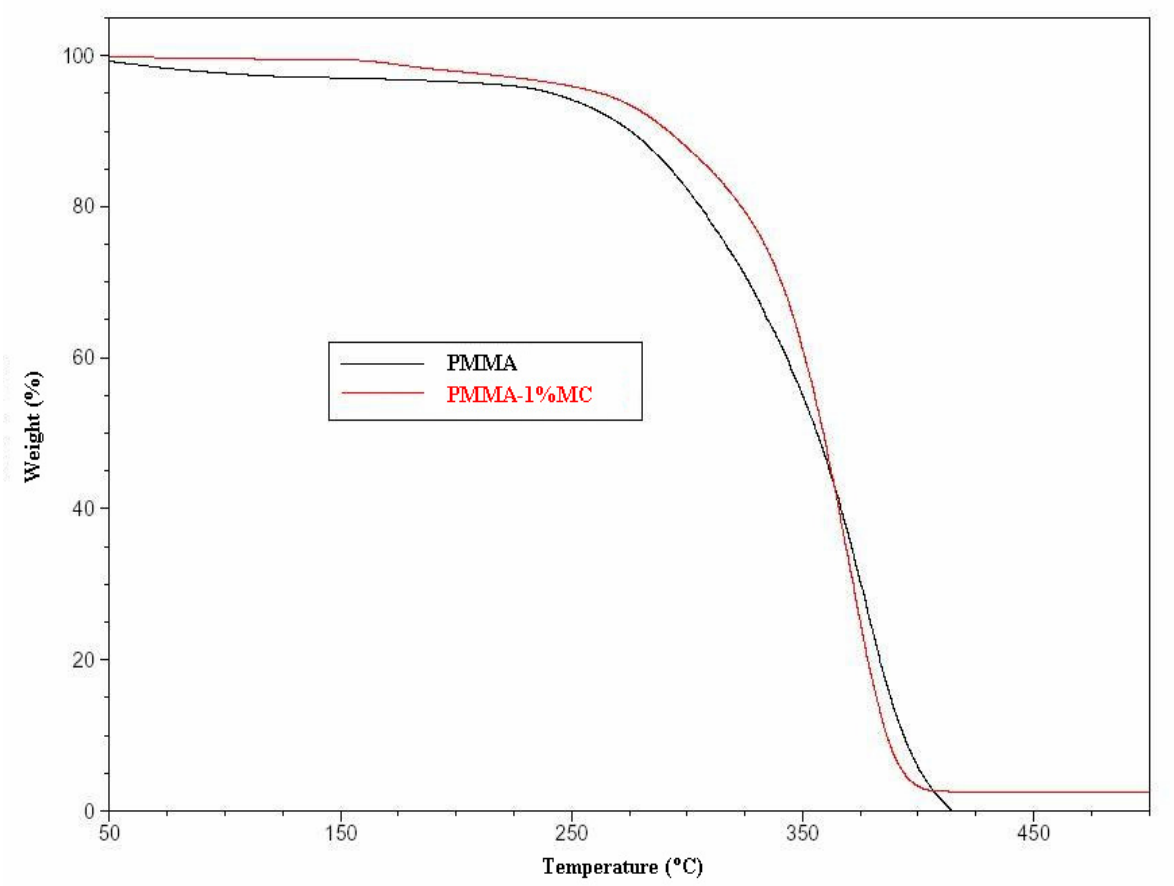

Figure 3.7 TGA graphs of PMMA and PMMA-1%MC

The increase in T_g of PMMA with nanocomposite formation (Figure 3.8) can be ascribed to its exfoliation morphology with fine dispersion of organo-clay particles in the polymer matrix that provides large surface area for clay interacting with polymer matrix, which can then lead to the restricted segmental motions near the organic–inorganic interfaces [96].

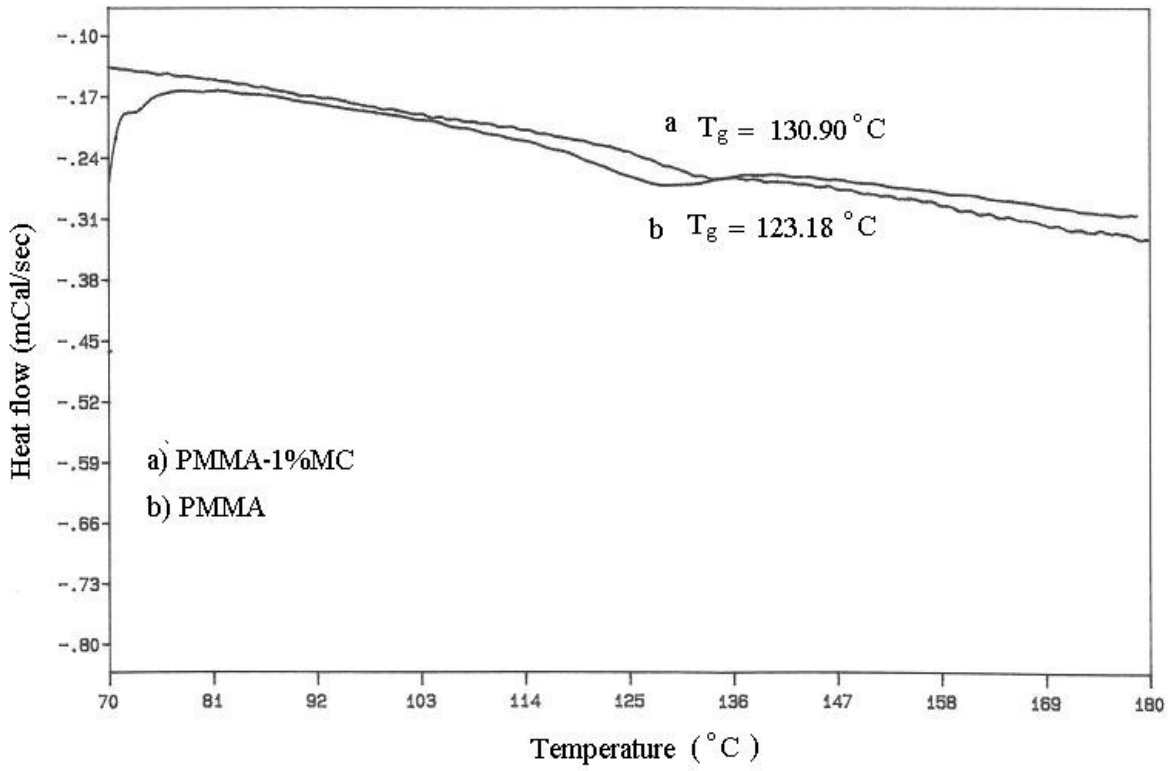

Figure 3.8 DSC graphs of PMMA and PMMA-1%MC

The exfoliation trend of the clay in PMMA-1%MC nanocomposite was also confirmed by TEM (Figure 3.9). Grey background belongs to the polymer matrix and the darker lines correspond to the silicate platelets. Any micron-sized silicates were not observed in the image. However, the dispersed silicate nanoplatelets, with high aspect ratios and thickness less than 20 nm, are clearly observed. The well dispersion of clay platelets in PMMA matrix resulted from the efficient intragallery over extra-gallery polymerization, owing to the anchored photoinitiator and monomer in the interlayer space of clay layers. As there is a disordered dispersion of clay layers in the polymer matrix and there is no clay particles thicker than 20 nm, it can be said that PMMA-1%MC exhibits an exfoliated structure [86]. This observation is also consistent with the XRD results assigning the exfoliation to the same composite.

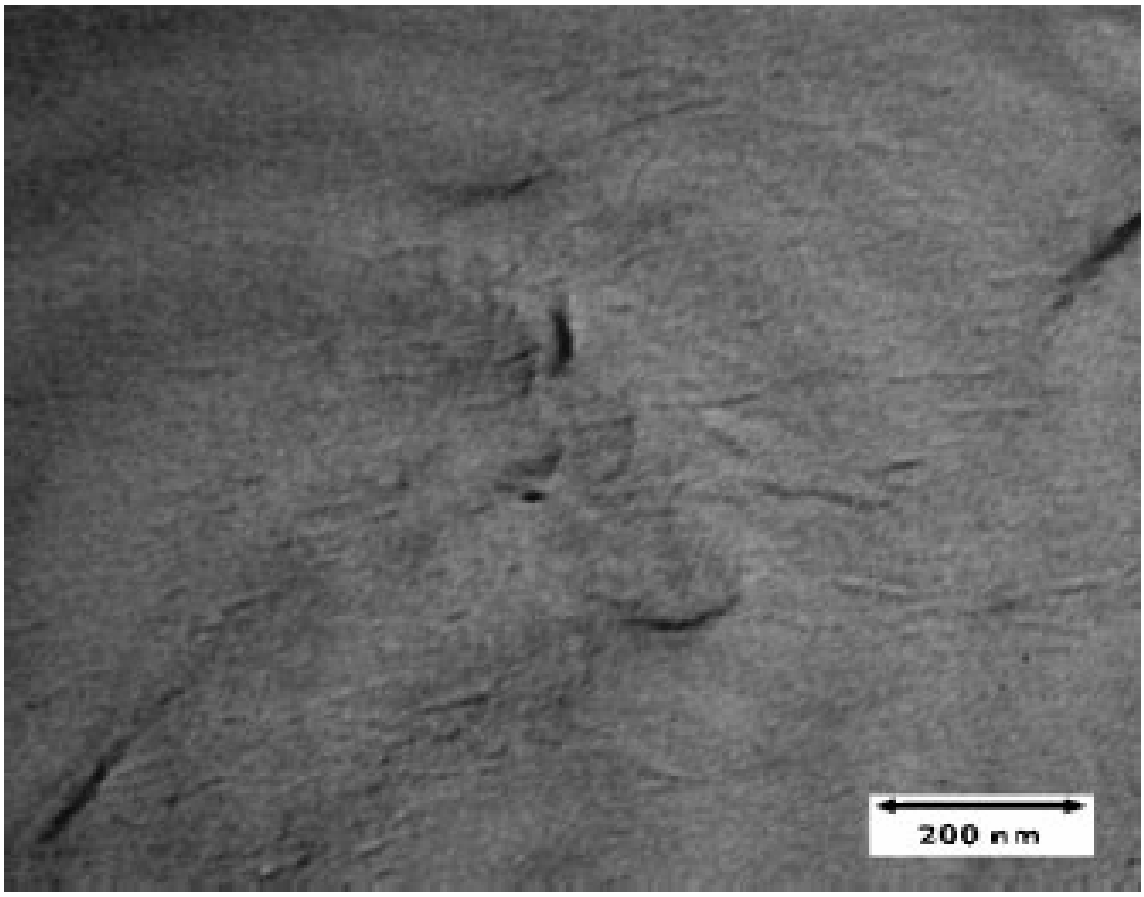

Figure 3.9 TEM image of PMMA-1%MC

3.4 Effect of Loading Degree on Nanocomposite Properties

In order to investigate the effect of loading on the performance of nanocomposites, other compositions were prepared and characterized. In Figure 3.10 XRD patterns of PMMA-1%MC, PMMA-3%MC and PMMA-5%MC are given and their XRD data are summarized in Table 3.2.

Two of the resulting nanocomposites obtained from MC, PMMA-3%MC and PMMA-5%MC were found to cause only a further increase in d-spacing of the MMT layers in MC indicating an intercalated nanocomposite structure.

On the other hand, as it was previously pointed out that, the nanocomposite PMMA-1%MC was found to result in an exfoliated structure which is confirmed with the

absence of any d_{001} reflection in the XRD pattern. The existence of exfoliation may be due to good compatibility of PMMA with monomer at low concentration. It might result from the interaction of clay surface with polar groups in PMMA [97]. Based on this information, at higher loadings it seems that there might be relatively more attractive forces between the clay layers which may lead to some intercalated tactoids with a small peak in XRD patterns [58].

Table 3.2 XRD data results of clays and nanocomposites

Clays and nanocomposites	d_{001} of clay (Å)
NaMMT	12.13
MC	17.11
PMMA-1%MC	No Reflection
PMMA-3%MC	15.50
PMMA-5%MC	15.76

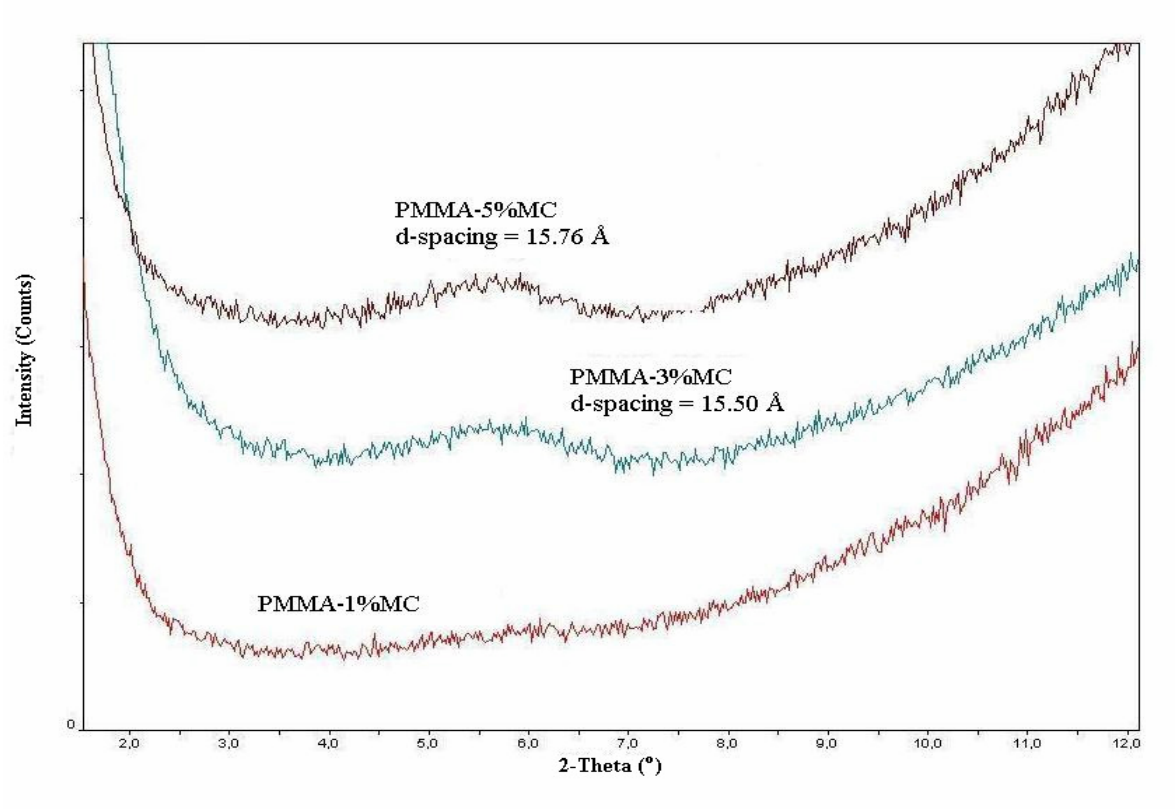

Figure 3.10. XRD patterns of nanocomposites

The TGA graphs of neat PMMA and the nanocomposites given in Figure 3.11 clearly show that all the nanocomposites exhibited enhanced thermal stabilities compared to pure PMMA. Both the decomposition onset and mid-point degradation temperatures of the nanocomposite PMMA-1%MC shifted toward the higher temperatures as compared to neat PMMA, PMMA-3%MC and PMMA-5%MC nanocomposites. This result indicates that the exfoliated nanocomposite (PMMA-1%MC) is more stable than the others, most probably due to the maximized interaction between the clay and the polymer in an exfoliated nanocomposite structure resulting from the availability of larger surface area of clay for polymer matrix [30]. It leads to restricted thermal motions of the PMMA molecules near the clay surface. On the other hand, as it can be seen from the figure that both intercalated nanocomposites, PMMA-3%MC and PMMA-5%MC have higher decomposition onset temperatures compared to neat PMMA indicating that thermal stability of PMMA increases with MMT loading. This result is in agreement with the fact that intercalated nanocomposites are known to have higher thermal stabilities than that of pure polymer due to the convoluted path formed in the intercalated structures [6].

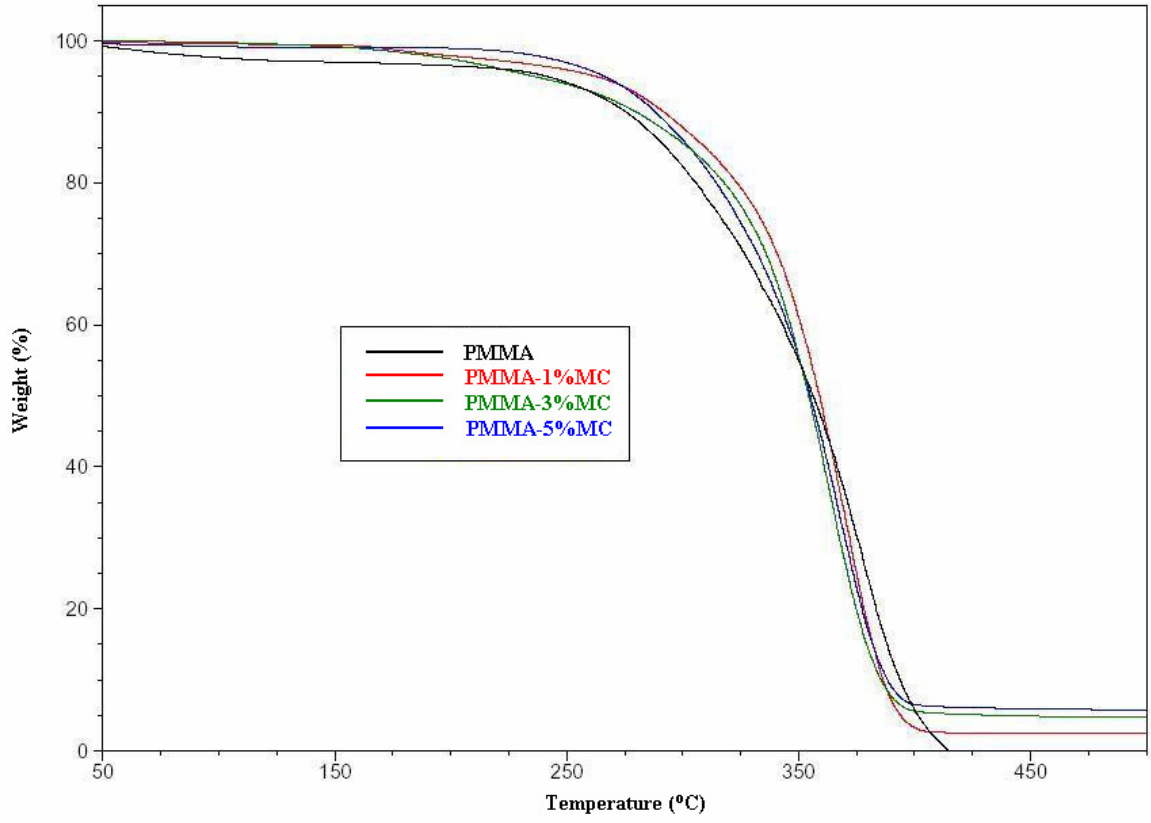

Figure 3.11. TGA graphs of PMMA and nanocomposites

All the PMMA nanocomposites show a higher T_g compared to neat PMMA as given in DSC thermograms in Figure 3.12. The highest increase in T_g is observed for PMMA-1%MC nanocomposite. This can be attributed to its exfoliation morphology with fine dispersion of organo-clay particles in the polymer matrix which provides large surface area for clay interacting with polymer matrix which in turn leading to segmental motions near the organic–inorganic interfaces being confined.

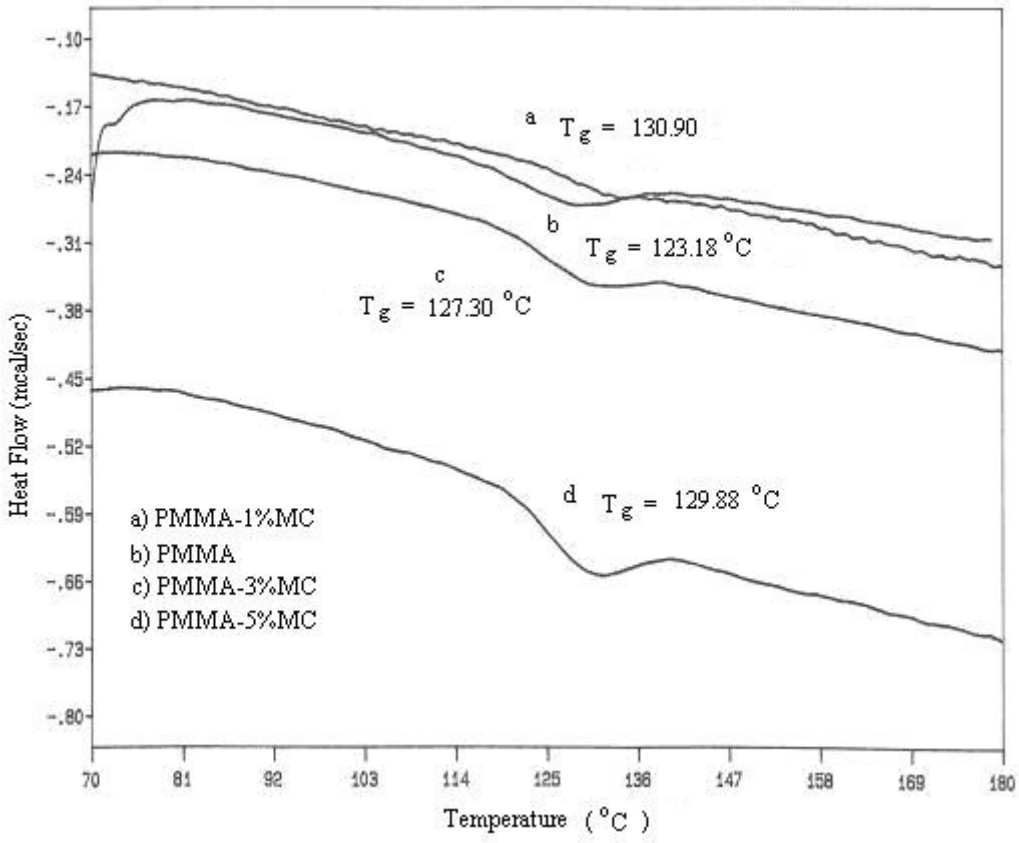

Figure 3.12 DSC graphs of PMMA and nanocomposites

Fracture surfaces of selected PMMA nanocomposites were investigated by SEM using backscattered imaging. The SEM images of PMMA-3%MC and PMMA-1%MC are chosen for the comparison in terms of intercalated and exfoliated structures, respectively. Figure 3.13 and Figure 3.14 show low-magnification microstructures in which the bright regions correspond to clay aggregates. In Figure 3.13, one can see big aggregated particles (ca.11.11 μm) together with small aggregates, which may be attributed to intercalated or partially exfoliated structure of the nanocomposite PMMA-3%MC. This may be most

probably due to the poor interaction of MC layers with polymer matrix in the interlayer galleries. On the other hand, in Figure 3.14 PMMA-1%MC as exfoliated nanocomposite has only small clusters of the clay particles (ca. 1.18 μm) that are homogeneously dispersed in the PMMA matrix.

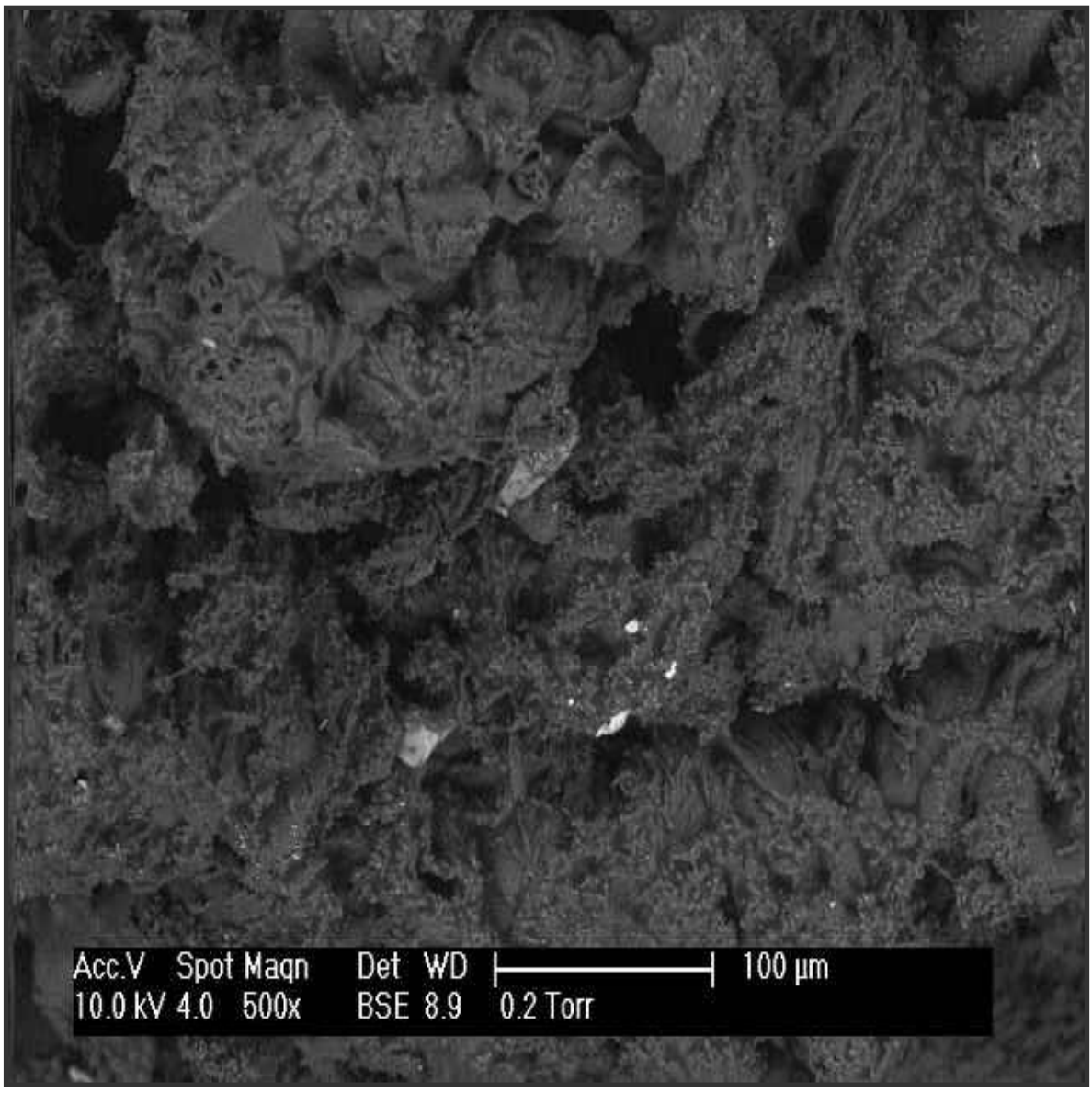

Figure 3.13 SEM image of fracture surface of PMMA-3%MC

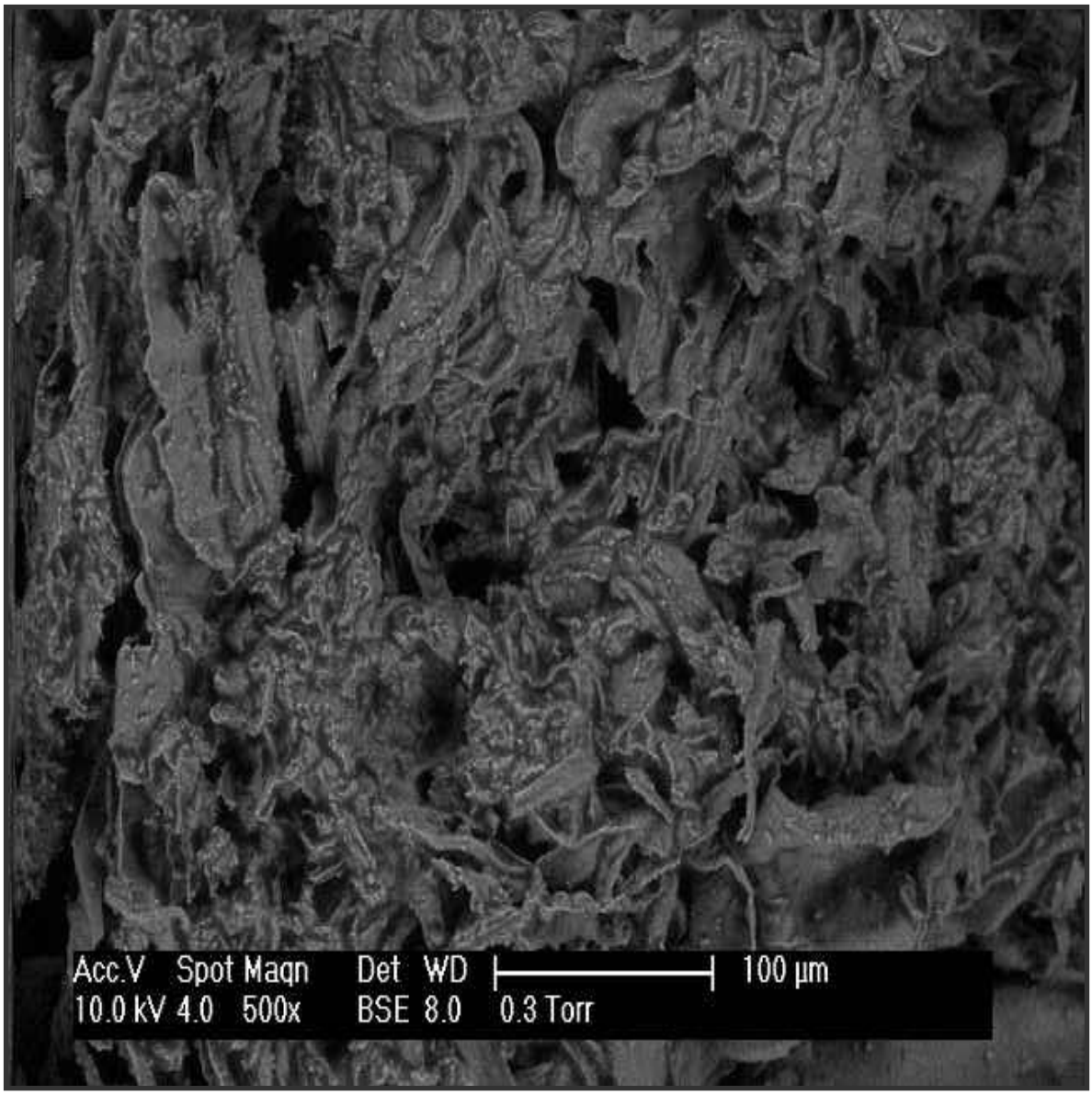

Figure 3.14 SEM image of fracture surface of PMMA-1%MC

4. CONCLUSIONS

In this study, a novel approach which is based on the intercalation of the photoinitiator moiety through quaternized ammonium ions present in the photoinitiator structure to prepare clay-PMMA nanocomposite was introduced. Polymerization through the interlayer galleries of clay was achieved by photoinduced decomposition of the intercaler-initiator (PDA).

Intercalation ability of the photoinitiator was evidenced by XRD technique. XRD patterns showed that the intercalation of MMT layers with the photoinitiator caused about a 5 Å increase in d-spacing of MMT layers that is a proof of intercalated photoinitiator. By this way, it was proved that polymerization reaction can occur in between MMT layers that is the main target of many polymer-nanocomposite studies.

Correlation of the intercalation-exfoliation behavior of nanocomposite with different degrees of MC loadings were examined. It was found that exfoliation/intercalation structures were closely related with loading degree. The exfoliation target has been reached with 1 % loading of MC whereas other loading degrees resulted in complete intercalation.

Moreover, thermal stability examined by TGA analyses claimed that the most stable nanocomposite is the one which contains 1 % MC with the highest decomposition onset and mid-point degradation temperatures compared to both intercalated ones and PMMA itself.

Compared to neat PMMA, all nanocomposites exhibited higher T_g values in their DSC analyses. It was also clear that exfoliated nanocomposite has also the highest T_g which is, in turn, has the highest stiffness.

SEM images of fracture surfaces of PMMA-3%MC and PMMA-1%MC composites showed different sizes of clay aggregates as bright regions. The existence of relatively bigger clay aggregates in the intercalated nanocomposites and smaller ones for

exfoliated nanocomposite in their images were found to be in good agreement with their XRD, TGA and DSC results.

This approach opens new pathways for the clay-polymer composites designing intercalating agents capable of initiating polymerization of appropriate monomers by means of various external stimulation such as heat, light, *etc.*

REFERENCES

1. Wang, T. and A. Mezzatesta, "3-D DC Resistivity Modeling Using the Sweeping-Seed, Conjugate-Gradient Method", *Geophysics*, Vol. 66, pp. 441-447, 2001.

2. Brune, D.A., and J. Bicerano, "Micromechanics of Nanocomposites: Comparison of Tensile and Compressive Elastic Moduli, and Prediction of Effects of Incomplete Exfoliation and Imperfect Alignment on Modulus", *Polymer*, Vol. 43, pp. 369-374, 2002.

3. Luo, J. J. and I. M. Daniel, "Characterization and Modeling of Mechanical Behavior of Polymer/Clay Nanocomposites", *Composites Science and Technology*, Vol. 63, pp. 1607-1616, 2003.

4. Fornes, T. D. and D.R. Paul, "Modeling Properties of Nylon 6/Clay Nanocomposites Using Composite Theories", *Polymer*, Vol. 17, pp. 4993-5013, 2003.

5. Gao, F., "Clay/Polymer Composites: the Story", *Materials Today*, Vol. 7, pp. 50-55, 2004.

6. Ray, S. S. and M. Okamoto, "Polymer/Layered Silicate Nanocomposites: a Review From Preparation to Processing", *Progress in Polymer Science*, Vol. 11, pp. 1539-1641, 2003.

7. Kojima, Y., A. Usuki, M. Kawasumi, A. Okada, T. Kurauchi, O. Kamigaito, "One-Pot Synthesis of Nylon 6-Clay Hybrid", *Journal of Polymer Science Part A: Polymer Chemistry*, Vol. 31, pp. 1755-1758, 1993.

8. Gilman, J. W., "Flammability and Thermal Stability Studies of Polymer Layered-Silicate (Clay) Nanocomposites", *Applied Clay Science*, Vol. 15, pp. 31-49, 1999.

9. Marosföi, B., S. Matko and P. Anna G. Marosi, "Fire Retarded Polymer Nanocomposites", *Current Applied Physics*, Vol. 6, pp. 259-261, 2006.

10. Yano, K., A. Usuki, A. Okoda, T. Kuruachi, O. Kamigaito, "Synthesis and Properties of Polyimide-Clay Hybrid", *Journal of Polymer Science Part A: Polymer Chemistry*, Vol. 31, pp. 2493-2498, 1993.

11. Nah, C., H. J. Ryu, W. D. Kim, S. S. Choi, "Barrier Property of Clay/Acrylonitrile-Butadiene Copolymer Nanocomposite", *Polymers for Advanced Technologies*, Vol. 13, pp. 649-652, 2002.

12. Gorrasi, G., M. Tortora, V. Vittoria, E. Pollet, B. Lepoittevin, M. Alexandre and P. Dubois, "Vapor Barrier Properties of Polycaprolactone Montmorillonite Nanocomposites: Effect of Clay Dispersion", *Polymer*, Vol 44, pp. 2271-2279, 2003.

13. Vaia, R. A., S. Vasudevan, W. Krawiec, G. Lawrence, P. Giannelis, "New Polymer Electrolyte Nanocomposites: Melt Intercalation of Poly(ethylene oxide) in Mica-Type Silicates", *Advanced Materials*, Vol. 7, pp. 154-156, 1995.

14. Hutchison, J. C., R. Bissessur and D. F. Shriver, "Conductivity Anisotropy of Polyphosphazene-Montmorillonite Composite Electrolytes", *Chemistry of Materials*, Vol. 8, pp. 1597-1599, 1996.

15. Edser, C., "Auto Applications of Drive Commercialization of Nanocomposites", *Plastic Additives & Compounding*, Vol. 4, pp. 30-33, 2002.

16. Cox, H., T. Dearlove, W. Rodges, M. Verbrugge, C. S. Wang, "Nanocomposite Systems for Automotive Applications", *4th World Congress in Nanocomposites*, EMC, San Francisco, 1-3 September 2004.

17. Patterson, T., "Nanocomposites – Our Revolutionary Breakthrough", *4th World Congress in Nanocomposites*, EMC, San Francisco, 1-3 September 2004.

18. Goldman, A. Y. and C. J. Copsey, "Multilayer Barrier Liner Material With Nanocomposites for Packaging Applications", *4th World Congress in Nanocomposites*, EMC, San Francisco, 1-3 September 2004.

19. Conway, R., "Using Nanotechnology to Provide Active and Passive Barriers in Beverage Packaging Application", *The Future of Nanomaterials Conference*, Pira, Birmingham, 29-30 June 2004.

20. Radford, J., "Enhanced Barrier Properties in Containers and Films", *The Future of Nanomaterials Conference*, Pira, Birmingham, 29-30 June 2004.

21. Okada, A., M. Kawasumi, A. Usuki, Y. Kojima, T. Kurauchi, O. Kamigaito, "Synthesis and Properties of Nylon-6/Clay Hybrids", *MRS Symposium Proceedings*, Pittsburgh, Vol. 171, pp. 45–50, 1990.

22. Giannelis, E. P., " Polymer Layered Silicate Nanocomposites", *Advanced Materials*, Vol. 8, pp. 29–35, 1996.

23. Giannelis, E.P., R. Krishnamoorti., E. Manias, "Polymer-Silicate Nanocomposites: Model Systems for Confined Polymers and Polymer Brushes", *Advanced Polymer Science*, Vol.138, pp. 107–47, 1999.

24. Le Baron, P. C., Z. Wang, T. J. Pinnavaia, "Polymer-Layered Silicate Nanocomposites: an Overview", *Applied Clay Science*, Vol. 15, pp. 11–29, 1999.

25. Vaia, R. A., G. Price, P. N. Ruth, H. T. Nguyen, J. Lichtenhan, "Polymer/Layered Silicate Nanocomposites as High Performance Ablative Materials", *Applied Clay Science*, Vol. 15, pp. 67–92, 1999.

26. Biswas, M., S. S. Ray, "Recent Progress in Synthesis and Evaluation of Polymer–Montmorillonite Nanocomposites", *Advanced Polymer Science*, Vol. 155, pp. 167–221, 2001.

27. Brindly, S.W., G. Brown, “Crystal Structure of Clay Minerals and Their X-Ray Diffraction”, *Chemical Geology*, Vol. 33, pp. 369-370, 1981.

28. Aranda, P. and E. Hitzky, “Poly(ethylene oxide)-Silicate Intercalation Materials”, *Chemistry of Materials*, Vol. 4, pp. 1395–403, 1992.

29. Greenland, D. J., “Adsorption of Poly(vinyl alcohols) by Montmorillonite”, *Journal of Colloid Science*, Vol 18, pp. 647–64, 1963.

30. Blumstein, A., “Polymerization of Adsorbed Monolayers: II. Thermal Degradation of the Inserted Polymers”, *Journal of Polymer Science Part A: Polymer Chemistry*, Vol. 3, pp. 2665–2673, 1965.

31. Vaia, R. A. and E. P. Giannelis, “Structure and Dynamics of Polymer-Layered Silicate Nanocomposites”, *Chemistry of Materials*, Vol. 8, pp. 1728–1734, 1996.

32. Lagaly, G., “Interaction of Alkylamines With Different Types of Layered Compounds”, *Solid State Ionics*, Vol. 22, pp. 43–51, 1986.

33. Vaia R. A., R. K. Teukolsky, E. P. Giannelis, “Interlayer Structure and Molecular Environment of Alkylammonium Layered Silicates”, *Chemistry of Materials*, Vol. 6, pp. 1017–1022, 1994.

34. Ray, S. S., K. Okamoto, M. Okamoto, “Structure–Property Relationship in Biodegradable Poly(butylene succinate)/Layered Silicate Nanocomposites”, *Macromolecules*, Vol. 36, pp. 2355–2367, 2003.

35. Okada, A., A. Usuki, T. Kurauchi and O. Kamigaito, “Polymer-Clay Hybrids, Hybrid Organic-Inorganic Composites”, *American Chemical Society*, Vol. 7, pp. 55-65, 1995.

36. Kojima, Y., A. Usuki, M. Kawasumi, A. Okada, T. Kurauchi, O. Kamigaito and K. Kaji, "Novel Preferred Orientation in Injection - Molded Nylon 6 - Clay Hybrid", *Journal of Polymer Science Part B: Polymer Physics*, Vol. 33, pp. 1039-1045, 1995.

37. Okada, A., M. Kawasumi, A. Usuki, Y. Kojima, T. Kurauchi, and O. Kamigaito, "Nylon-6/Clay Hybrid", *Materials Research Society Proceedings*, Vol. 171, pp. 45-50, 1990.

38. Lemmon, J. P., J. Wu, C. Oriakhi and M. M. Lerner, "Preparation of Nanocomposites Containing Poly(ethylene oxide) and Layered Solids", *Electrochimica Acta*, Vol. 40, pp. 2245-2249, 1995.

39. Biasci, L., M. Aglietto, G. Ruggeri and F. Ciardelli, "Functionalization of Montmorillonite by Methyl Methacrylate Polymers Containing Side-Chain Ammonium Cations", *Polymer*, Vol. 35, pp. 3296-3304, 1994.

40. Moet, A., A. Akelah, N. Salahuddin, A. Hiltner, and E. Baer, "Layered Silicate/ATBN Nanocomposite", *Materials Research Society Proceedings*, Vol. 351, pp. 163-170, 1994.

41. Messersmith, P. B. and E. P. Giannelis, "Synthesis and Barrier Properties of Poly(ε-caprolactone)-Layered Silicate Nanocomposites", *Journal of Applied Polymer Science Part A: Polymer Chemistry*, Vol. 33, pp. 1047-1057, 1995.

42. Vaia, R., A. H. Ishii and E. P. Giannelis, "Synthesis and Properties of Two-Dimensional Nanostructures by Direct Intercalation of Polymer Melts in Layered Silicates", *Chemistry of Materials*, Vol. 5, pp. 1694-1696, 1993.

43. Moet, A., A. Akelah, A. Hiltner and E. Baer, "Layered Silicate/Polystyrene Nanocomposite", *Materials Research Society Proceedings*, Vol. 351, pp. 91-96, 1994.

44. Pinnavaia, T. J., T. Lan, P. D. Kaviratna and M. S. Wang, "Clay-Polymer Nanocomposites: Polyether and Polyimide Systems", *Materials Research Society Proceedings*, Vol. 346, pp. 81-87, 1994.

45. Yano, K., A. Usuki and A. Okada, "Synthesis and Properties of Polyimide-Clay Hybrid Films", *Journal of Polymer Science Part A: Polymer Chemistry*, Vol. 35, pp. 2289-2294, 1997.

46. Ke, Y., C. Long and Z. Qi, "Crystallization, Properties and Crystal and Nanoscale Morphology of PET-Clay Nanocomposites", *Journal of Applied Polymer Science*, Vol. 71, pp. 1139-1146, 1999.

47. Usuki, A., M. Kato, A. Okada and T. Kurauchi, "Synthesis of Polypropylene-Clay Hybrid", *Journal of Applied Polymer Science*, Vol. 63, pp. 137-139, 1997.

48. Kato, M., A. Usuki and A. Okada, "Synthesis of Polypropylene Oligomer-Clay Intercalation Compounds", *Journal of Applied Polymer Science*, Vol. 66, pp. 1781-1785, 1997.

49. Hasegawa, N., M. Kawasumi, M. Kato, A. Usuki and A. Okada, "Preparation and Mechanical Properties of Polypropylene-Clay Hybrids Using a Maleic Anhydride-Modified Polypropylene Oligomer", *Journal of Applied Polymer Science*, Vol. 67, pp. 87-92, 1998.

50. Kawasumi, M., N. Hasegawa, M. Kato, A. Usuki, and A. Okada, "Preparation and Mechanical Properties of Polypropylene-Clay Hybrids", *Macromolecules*, Vol. 30, pp. 6333-6338, 1997.

51. Lan, T. and T. J. Pinnavaia, "Clay-Reinforced Epoxy Nanocomposites", *Chemistry of Materials*, Vol. 6, pp. 2216-2219, 1994.

52. Kelly, P., A. Akelah, S. Qutubuddin, and A. Moet, "Reduction of Residual Stress in Montmorillonite/Epoxy Compounds", *Journal of Materials Science*, Vol. 29, pp. 2274-2280, 1994.

53. Messersmith, P. B. and E. P. Giannelis, "Synthesis and Characterisation of Layered Silicate-Epoxy Nanocomposites", *Chemistry of Materials*, Vol. 6, pp. 1719-1725, 1994.

54. Wang, Z. and T. J. Pinnavaia, "Nanolayer Reinforcement of Elastomeric Polyurethane", *Chemistry of Materials*, Vol. 10, pp. 3769-3771, 1998.

55. Zilg, C., R. Thomann, R. Mulhaüpt and J. Finter, "Polyurethane Nanocomposites Containing Laminated Anisotropic Nanoparticles Derived from Organophilic Layered Silicates", *Advanced Materials*, Vol. 11, pp. 49-51, 1999.

56. Burnside, S. D. and E. P. Giannelis, "Synthesis and Properties of New Poly(dimethylsiloxane) Nanocomposites", *Chemistry of Materials*, Vol. 7, pp. 1597-1600, 1995.

57. Wang, S., C. Long, X. Wang, Q. Li and Z. Qi, "Synthesis and Properties of Silicone/ Organo-Montmorillonite Hybrid Nanocomposites", *Journal of Applied Polymer Science*, Vol. 69, pp. 1557-1561, 1998.

58. Lan, T., P. D. Kaviratna and T. J Pinnavaia, "Mechanism of Clay Tactoid Exfoliation in Epoxy-Clay Nanocomposites", *Chemistry of Materials*, Vol. 7, pp. 2144-2150, 1995.

59. Ke, Y., C. Long and Z. Qi, "Crystallization, Properties and Crystal and Nanoscale Morphology of PET-Clay Nanocomposites", *Journal of Applied Polymer Science*, Vol. 71, pp. 1139-1146, 1999.

60. Vaia, R. A. and E.P. Giannelis, “Lattice of Polymer Melt Intercalation in Organically-Modified Layered Silicates”, *Macromolecules*, Vol. 30, pp. 7990–7999, 1997.

61. Francis, C. W., “Adsorption of Polyvinylpyrrolidone on Reference Clay Minerals”, *Soil Science Society of America Journal*, Vol. 115, pp. 40–54, 1973.

62. Zhao, X., K. Urano and S. Ogasawara, “Adsorption of Poly(ethylene vinyl alcohol) From Aqueous Solution on Montmorillonite Clays”, *Colloid and Polymer Science*, Vol. 267, pp. 899–906, 1989.

63. Jimenez, G., N. Ogata, H. Kawai, T. Ogihara, “Structure and Thermal/Mechanical Properties of Poly(1 -caprolactone)–Clay Blend”, *Journal of Applied Polymer Science*, Vol. 64, pp. 2211–2220, 1997.

64. Ogata, N., Jimenez G, Kawai H, Ogihara T., “Structure and Thermal/Mechanical Properties of Poly(L-lactide)–Clay Blend”, *Journal of Polymer Science Part B: Polymer Physics*, Vol. 35, pp. 389–396, 1997.

65. Jeon, H. G., H. T. Jung, S. W. Lee, S. D. Hudson, “Morphology of Polymer Silicate Nanocomposites. High Density Polyethylene and a Nitrile”, *Polymer Bulletin*, Vol. 41, pp. 107–113, 1998.

66. Kawasumi, M., N. Hasegawa, A. Usuki, A. Okada, “Nematic Liquid Crystal/Clay Mineral Composites”, *Materials Science and Engineering*, Vol. 6, pp. 135–143, 1998.

67. Alexandre, M., and P. Dubois, “Polymer-Layered Silicate Nanocomposites: Preparation, Properties and Uses of a New Class of Materials”, *Materials Science and Engineering*, Vol. 28, pp. 1-63, 2000.

68. Liu, L., Z. Qi and X. Zhu, "Studies on Nylon 6/Clay Nanocomposites by Melt-Intercalation Process", *Journal of Applied Polymer Science*, Vol. 71, pp. 1133-1138, 1999.

69. Vaia, R. A., K. D. Jandt, E. J. Kramer and E. P. Giannelis, "Microstructural Evolution of Melt Intercalated Polymer-Organically Modified Layered Silicates Nanocomposites", *Chemistry of Materials*, Vol. 8, pp. 2628-2635, 1996.

70. Morgan A.B., J. W. Gilman, "Characterization of Poly-Layered Silicate (Clay) Nanocomposites by Transmission Electron Microscopy and X-Ray Diffraction: a Comparative Study", *Journal of Applied Polymer Science*, Vol. 87, pp.1329–1338, 2003.

71. Schnabel, W., K. M. Mishra, O. Nuyken, S. Kobayashi, Y. Yağcı, "Photoinitiation of Ionic Polymerization", *Macromolecular Engineering: Recent Aspects*, pp. 67-83, Plenum Press, New York, 1995.

72. J. P. Fouassier, *Photoinitiation, Photopolymerization and Photocuring. Fundamentals And Applications*, Hanser Publishers, Munich, Vienna, New York, 1995.

73. Blyth, J. and A. W. Hoffmann, "Polymerization of Styrene by Sunlight", *Chemical Annuals*, Vol. 53, pp. 292-296, 1845.

74. Miller, C. W., E. S. Jönsson, C. E. Hoyle, K. Viswanathan and E. J. Valente, "Evaluation of N-Aromatic Maleimides as Free Radical Photoinitiators: A Photophysical and Photopolymerization Characterization", *Journal of Physical Chemistry Part B: Polymer Physics*, Vol. 105, pp. 2707-2717, 2001.

75. Decker, C., F. Morel, S. Jonsson, S. Clark, and C. Hoyle, "Light-Induced Polymerization of Photoinitiator-Free Vinyl Ether Maleimide Systems", *Macromolecular Chemistry and Physics*, Vol. 200, pp. 1005-1013, 1999.

76. Kohli, P., A. B. Scranton, and G. J. Blanchard,. "Co-Polymerization of Maleimides and Vinyl Ethers: A Structural Study", *Macromolecules*, Vol. 31, pp. 5681-5689, 1998.

77. Cai, Y. and J. L. P. Jessop, "Free Radical Photopolymerization", *Encyclopedia of Polymer Science and Technology*, John Wiley & Sons, New York, 2004.

78. Reetz, I., Y. Yağcı, M. K. Mishra,. "Photoinitiated Radical Vinyl Polymerization", *Handbook of Radical Vinyl Polymerization*, CRC press, New York, 1998.

79. Dietliker, K., "Chemistry and Technology of UV and EB Formulations For Coatings", *Inks And Paints*, Sita Technology Ltd., London, 1991.

80. Turro, N.J., *Modern Molecular Photochemistry*, The Benjamin/Cummerings Publishing Co., Menlo Park California, 1978.

81. Murov, S. L., *Handbook of Photochemistry*, Marcel Dekker Inc., New York, 1973.

82. Turro, N. J., *Modern Molecular Photochemistry*, The Benjamin/Cummerings Publishing Co. Inc., Menlo Park California, 1978.

83. Rehm, D. and A. Weller, "Kinetics of Fluorescence Quenching by Electron and H-Atom Transfer", *Israel Journal of Chemistry*, Vol. 8, pp. 259-263, 1970.

84. Yeh, J. M., S. J. Liou, Y. W. Chang, "Polyacrylamide-Clay Nanocomposite Materials Prepared by Photopolymerization with Acrylamide as an Intercalating Agent", *Journal of Applied Polymer Science*, Vol. 91, pp. 3489-3496, 2004.

85. Huimin, W., M. Minghua, J. Yongcai, L. Qingshan, Z. Xiaohong, W. Shikang, "A Study on the Preparation of Polymer/Montmorillonite Nano-Composite Materials by Photo-Polymerization", *Polymer International*, Vol. 51, pp. 7-11, 2002.

86. Uhl., F. M., S. P. Davuluri, S. C. Wong, D. C. Webster, "Organically Modified Montmorillonites in UV Curable Urethane Acrylate Films", *Polymer*, Vol. 45, pp. 6175-6187, 2004.

87. Zahoily, K, S. Benfahri, T. Bendaikha, J. Baron, C. Decker, "UV-Radiation Curing of Photoiniator-Free Formulations", *Proceedings of the RadTech European Conference*, Basel, 8 - 10 October 2001, pp. 583-567, Elsevier, Amsterdam, 2001.

88. Decker, C., K. Keller, L. Benfahri, S. Zahouily, T. Bendaikha, J. Baron, "Ultrafast Synthesis of Bentonite-Acrylate Nanocomposite Materials by UV-Radiation Curing", *Journal of Materials Science*, Vol. 37, pp. 4831-4838 , 2002.

89. Benfahri, S., C. Decker, L. Keller, K. Zahoily, "Synthesis of Clay Nanocomposite Materials by Light-Induced Crosslinking Polymerization", *European Polymer Journal*, Vol. 40, pp. 493-501, 2003.

90. Şen, S., M. Memeşa, T. Nugay, and N. Nugay, "Synthesis of Effective Poly(4-vinylpyridine) Nanocomposites: In-situ Polymerization from Edges/surfaces and Interlayer Galleries of Clay", *Polymer International*, Vol. 55, pp. 216-221, 2006.

91. Redmer, P., B. Jedrzejewska, M. Pietzak, B. Paczkowska, L. A. Linden, J. Paczkowski, "Ultrafast Synthesis of Nanocomposite Coatings by UV Curing of Clay- or Silica-Filled Resins", *Polymer*, Vol. 47, pp. 136-140, 2002.

92. Jianbo, D., D. Y. Sogah, "Intergallery Living Polymerization Using Silicate-Anchored Photoiniferter. A Versatile Preparatory Method for Exfoliated Silicate nanocomposites", *Macromolecules*, Vol. 39, pp. 1020-1028, 2006.

93. Kasapoğlu, F., A. Önen, N. Bıçak, Y. Yağcı, "Photoinitiated Cationic Polymerization Using a Novel Phenacylanilinium Salt", *Polymer*, Vol. 43, pp. 2575-2579, 2002.

94. Kasapoğlu, F., Y. Yağcı, "Photosensitized Cationic Polymerization by Using Phenacylanilinium Salt", *Macromolecular Rapid Communications*, Vol. 23, pp. 567-570, 2002.

95. Kasapoğlu, F., N. Arsu, M. Aydın, Y. Yağcı, "Photoinitiated Polymerization of Methyl Methacrylate by Using Phenacyl Onium Salts", *Journal of Photochemistry and Photobiology Part A: Chemistry*., Vol. 19, pp. 151-159, 2003.

96. Landry, C. J. T., B. K. Coltrain, M. R. Landry, J. J. Fitzgerald, V. K. Long, "Poly(vinyl acetate)/Silica-Filled Materials: Material Properties of In Situ vs Fumed Silica Particles", *Macromolecules*, Vol. 26, 3702-3712, 1993.

97. Neşe, A., S. Şen, M. A. Taşdelen, N. Nugay, Y. Yağcı, "Clay-PMMA Nanocomposites by Photoinitiated Radical Polymerization Using Intercalated Phenacyl Pyridinium Salt Initiators", *Macromolecular Chemistry and Physics*, Vol. 207, pp. 820-826, 2006